9

Global Ventricular Function and Hemodynamics

ANDRÉ Y. DENAULT, PIERRE COUTURE
University of Montreal, Montreal, Canada

JEAN BUITHIEU
McGill University, Montreal, Canada

Important roles of perioperative transesophageal echocardiography (TEE) include the determination of baseline ventricular function before a surgical procedure and the identification of changes in ventricular function during cardiac and noncardiac procedures which in some cases may lead to severe hemodynamic instability which, when unresponsive to therapy, is considered a category 1 indication for the use of TEE (1). In such cases TEE allows precise determination of the mechanism of hemodynamic instability through evaluation of both left and right systolic and diastolic function.

I. NORMAL RIGHT AND LEFT VENTRICULAR MORPHOLOGY

The normal ventricular morphology and quantitative evaluation of ventricular size and function are described in Chapters 4 and 5 and in the American Society of Echocardiography (ASE) guidelines (2).

II. NORMAL RIGHT AND LEFT VENTRICULAR FUNCTION

A. Descent of the Base, Segmental Contraction, and Septal Curvature

There are several points which should be emphasized in the evaluation of normal ventricular function. Normal left ventricular function is associated with radial shortening but also longitudinal displacement of the base towards the apex by 15–20 mm which can be quantified using M-mode (3) or tissue Doppler imaging (4) and which correlates with ejection fraction (Fig. 9.1). There are normal regional variations in the thickening of ventricular segments with increasing contractility from the base to the apex. There is also rightward ventricular septal curvature because normal left ventricular pressure is generally superior to right ventricular pressure.

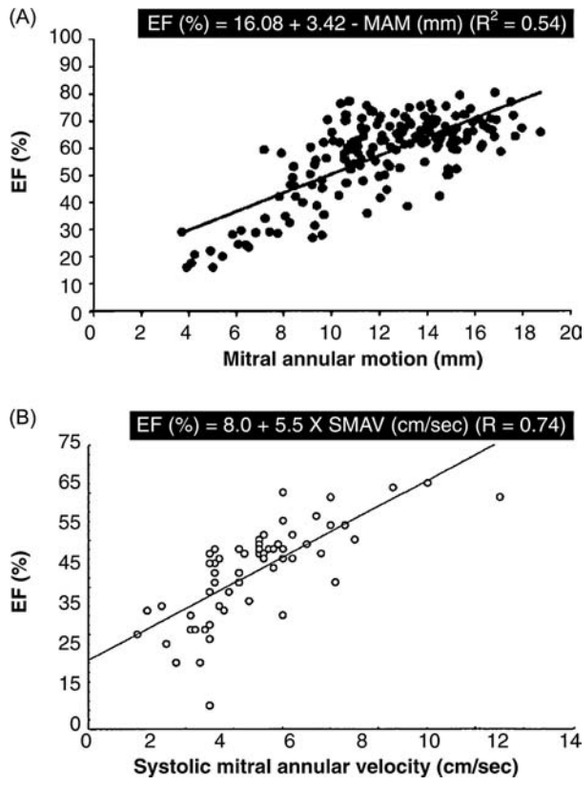

Figure 9.1 Relationship between ejection fraction (EF) and mitral annular motion (MAM) in 182 patients (A) and systolic mitral annular velocity (SMAV) by tissue Doppler in 60 patients (B). [Adapted with permission from Emilson et al. (3) and Alam et al. (4).]

B. Pressure–Volume Relationship

The determination of the relationship between ventricular function and hemodynamics is best described using the pressure–volume curves which allow graphical description of ventricular function by displaying a single cardiac cycle volume against pressure–time relationship (Fig. 9.2). This includes seven time-related events. Diastole starts with isovolemic relaxation (phase 4), continues with the opening of the mitral valve (MV) and early left ventricular filling, diastasis and atrial systole (phases 5–7) and ends with MV closure prior to isovolumic contraction (phase 1). Systole begins with the isovolumic contraction (phase 1), proceeds with the opening of the aortic valve (AoV) and ejection of the stroke volume (SV) (phases 2 and 3). The pressure–volume diagram can be obtained through continuous pressure and volume measurement but is rarely done in clinical practice.

Many determinants of the pressure–volume relationship may be obtained using TEE, a pulmonary artery catheter and a systemic arterial pressure catheter. Transesophageal echocardiography allows estimation of the volume component (or abscissa). Pressure components of the ordinate axis may be estimated from the pulmonary artery catheter and from systemic arterial pressure (Fig. 9.3). The left ventricular end-diastolic pressure (LVEDP) will be estimated by the pulmonary artery occlusion pressure (Paop) or wedge pressure at end-diastole, in the absence of any obstruction between the pulmonary capillary bed and the left ventricle (LV) such as mitral stenosis (MS). The left ventricular end-systolic pressure (LVESP) can be estimated by the systolic arterial pressure (SAP) if aortic valvular obstruction is absent (5,6). The left ventricular end-systolic volume (LVESV) and left ventricular end-diastolic volume (LVEDV) can be approximated by the left ventricular end-systolic area (LVESA) and left ventricular end-diastolic area (LVEDA) obtained from TEE short-axis transgastric views. The SV is calculated from the ratio of the thermodilution-derived cardiac output (CO) to the heart rate or through Doppler measurement (see Chapter 5). The area within the left ventricular pressure–volume curve is the left ventricular stroke work [LVSW = SV × (mean arterial pressure or MAP − Paop) × 0.0136] and this value is obtained through automated calculation of the cardiopulmonary profile.

Determinants of cardiac function, preload, afterload and contractility are easily plotted on the left ventricular pressure–volume relationships (Fig. 9.4). Each change in

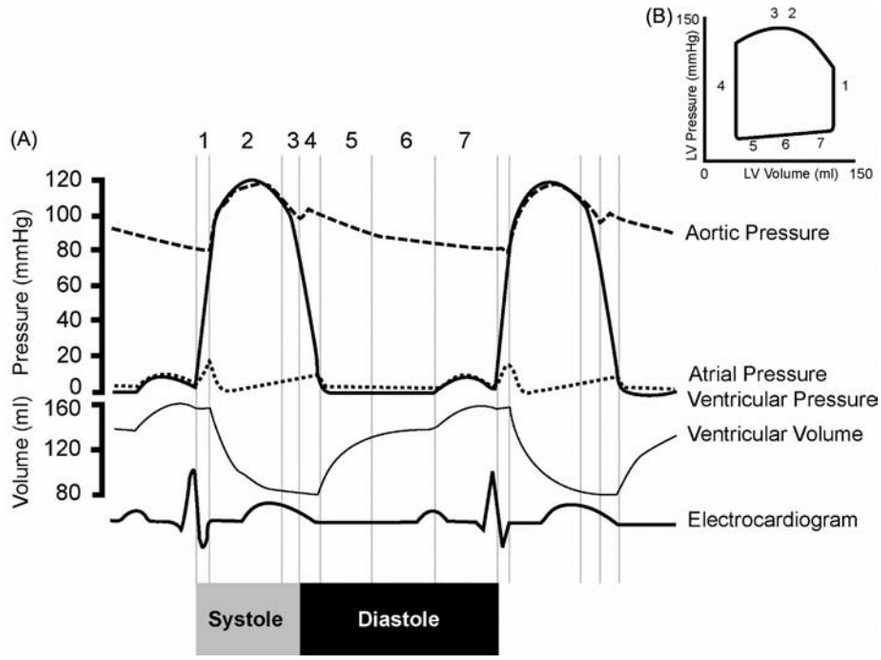

Figure 9.2 (A) Changes in aortic, atrial, ventricular pressure, and ventricular volume in relation to the electrocardiogram. Left ventricular (LV) pressure and volume over time during a cardiac cycle is characterized by seven time-related events. Isovolumic contraction [1] is followed by early [2] and late [3] ejection. Diastole starts with isovolumic relaxation [4] followed by the early filling phase after the opening of the mitral valve [5], diastasis [6], and atrial contraction [7]. (B) Corresponding LV pressure–volume relationship during one cardiac cycle.

these determinants will affect the pressure–volume relationship differently. In the following discussion, when possible, the effects of changes in cardiac function and their determinants will be explained by using the pressure–volume relationship.

1. Preload

A decrease in preload will be associated with a fall in LVEDV and LVEDP [Fig. 9.4(A)]. It is difficult clinically to differentiate between hypovolemia from reduced

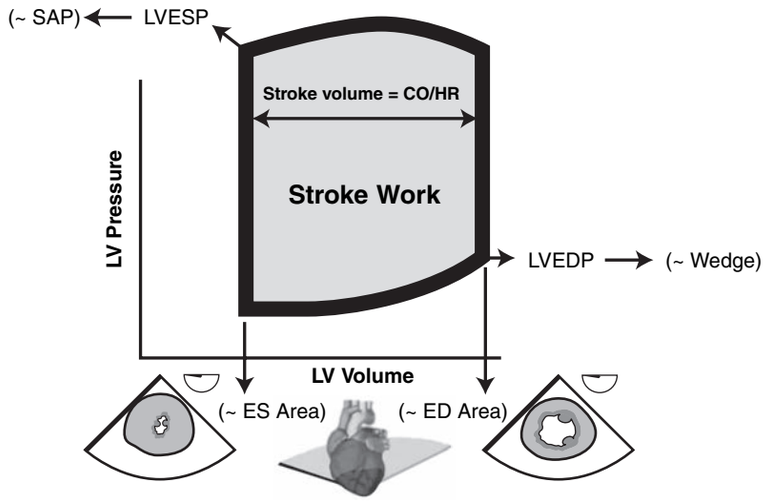

Figure 9.3 Left ventricular (LV) pressure–volume relationship during one cardiac cycle. The LV end-systolic pressure (LVESP) can be estimated using systolic arterial pressure (SAP) and the LV end-diastolic pressure (LVEDP) can be estimated with the pulmonary artery-derived "wedge" pressure at end-diastole. Using echocardiography, the LV end-systolic (ES) volume can be estimated with the ES area and the LV end-diastolic (ED) volume can be estimated with the ED area. The stroke volume, which is the difference between the ED volume and the ES volume, can be calculated from the ratio of the cardiac output (CO) obtained by Doppler or thermodilution divided by heart rate (HR). The LV stroke work corresponds to the area under the LV pressure–volume diagram (gray area). Changes in compliance of the left ventricle can explain why filling pressure does not always correlate with ventricular size.

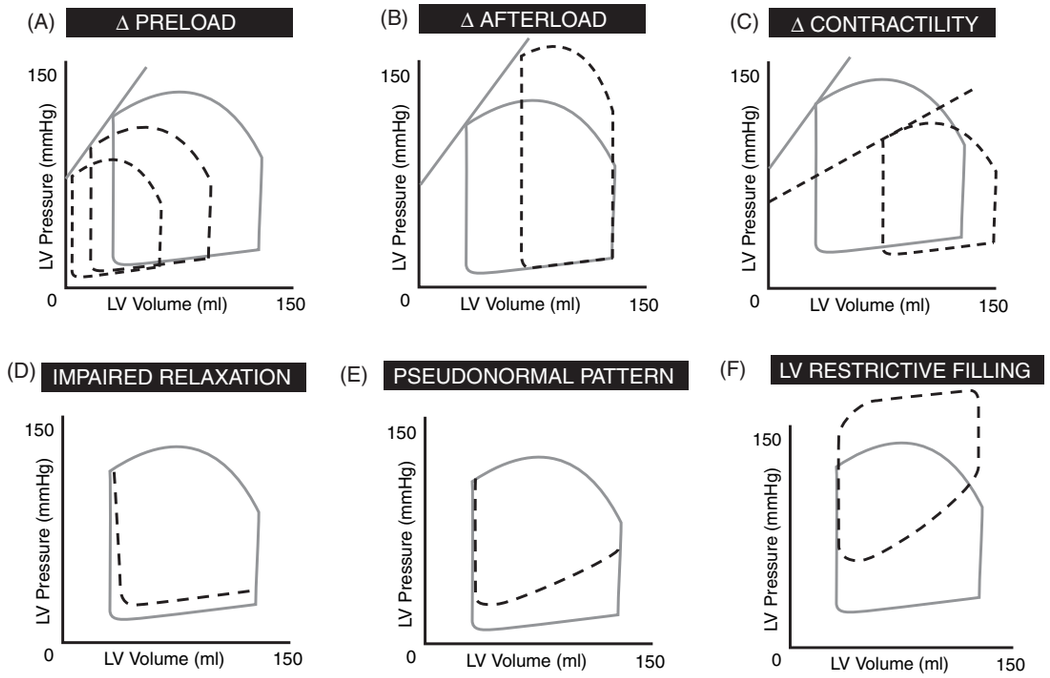

Figure 9.4 Left ventricular (LV) pressure–volume relationship showing changes in preload, afterload, contractility, and diastolic function. (A–C) Changes (Δ) in systolic function. (A) Decrease in preload: leftward and downward shift of the LV pressure–volume relationship with a reduction in end-diastolic pressure (EDP) and in end-diastolic volume (EDV). The elastance (left upper line) connects all the end-systolic points through which the pressure–volume diagram moves. (B) Increase in afterload: rightward and upward shift of the pressure–volume relationship with an increase in end-systolic pressure and in end-systolic volume. (C) Reduction in contractility: downward shift of the elastance with rightward displacement of the pressure–volume diagram. (D–F) Changes in diastolic function: with increasing severity, higher EDP is observed for the same EDV. (D) Stage I diastolic dysfunction: delayed LV relaxation. (E) Stage II diastolic dysfunction: pseudonormal filling pattern. (F) Stage III diastolic dysfunction: restrictive filling.

systemic vascular resistance (SVR) using TEE because both conditions will lead to reduction in preload. Both two-dimensional (2D) and Doppler indices have been used and validated to estimate left ventricular filling pressure and volume. Clinically useful echocardiographic 2D images for the diagnosis of hypovolemia or reduced SVR are the progressive reduction in LVEDA, left ventricular end-systolic cavity obliteration (Fig. 9.5), atrial septal displacement (Fig. 9.6) and both inferior and superior vena cava collapsibility (Fig. 9.7) (7), which will be discussed in the following text.

Left ventricular end-systolic cavity obliteration and its relationship to hypovolemia was studied by Leung et al. (8) in 139 patients undergoing cardiac surgery who were monitored continuously with TEE in the mid-papillary view. Hypovolemia, defined as a 10% reduction in LVEDA, was present in 80% of the observations of left ventricular end-systolic cavity obliteration. Consequently, this sign can occur in patients with increased ventricular performance, where a reduction in LVESV may be observed, without necessarily a reduction in LVEDV. Furthermore, the use of LVEDA as a predictor of responsiveness to increased preload has been shown to be limited (9–11). Kusumoto et al. (12) studied the atrial septal displacement as an index of reduced preload. As left atrial pressure is normally superior to right atrial pressure, the atrial septum should normally bulge towards the right atrium (RA) (convexity toward the RA) during most of the cardiac cycle (Fig. 9.6). In patients with mechanical ventilation, the authors observed that mid-systolic reversal of the atrial septal normal convexity occurred during expiration in 64 of 72 episodes when the wedge pressure was <15 mmHg and only two of 40 episodes when it was >15 mmHg. If the mid-systolic reversal of the atrial septum occurred during both inspiration and expiration, the wedge would usually be, <10 mmHg.

Another sign of preload responsiveness was described by Vieillard-Baron et al. (7). They observed that the presence of superior vena caval diameter collapse during

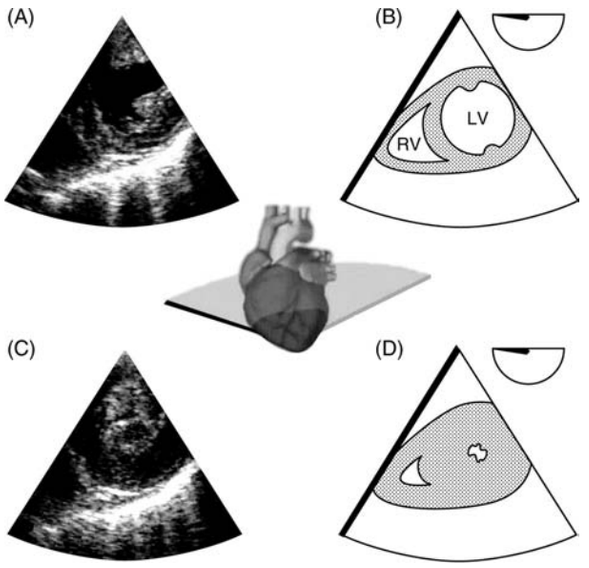

Figure 9.5 Left ventricular end-systolic cavity obliteration. Two-dimensional echocardiographic images of the left ventricle (LV) taken from a mid-papillary transgastric view during diastole (A, B) and systole (C, D). Example taken from an hypovolemic patient (RV, right ventricle).

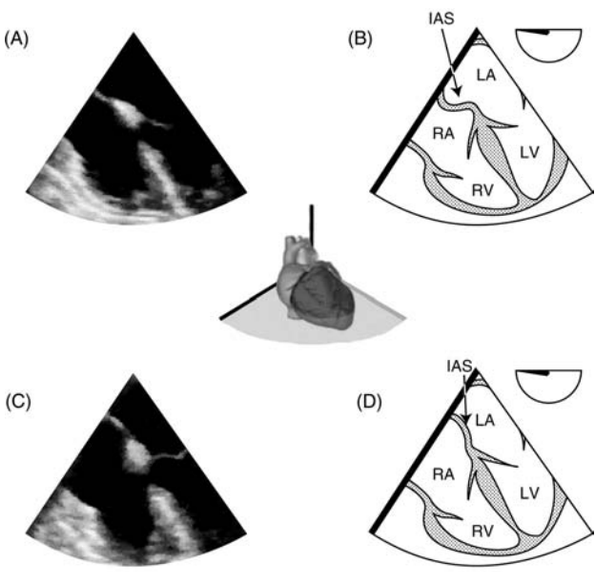

Figure 9.6 Using interatrial septal (IAS) displacement in the assessment of filling pressure. Mid-esophageal four-chamber view of the left ventricle (LV) in a patient following cardiopulmonary bypass. (A, B) The IAS deviated to the right: this implies that atrial pressure is higher on the left than on the right. The pulmonary artery occlusion pressure or "wedge" was 17 mmHg. (C, D) Following vasodilator therapy, the "wedge" pressure dropped to 7 mmHg. Now the IAS is displaced toward the left. This is consistent with the left atrial pressure being lower than the right (LA, left atrium; RA, right atrium; RV, right ventricle).

positive-pressure ventilation correlated with significant reduction in preload measured using Doppler velocities in the pulmonary artery. Using a collapsibility index, defined as the maximal expiratory diameter minus the minimal inspiratory diameter divided by the maximal diameter on expiration, patients with an index $>60\%$ had an inspiratory decrease in right ventricular outflow velocity close to 70%, as opposed to patients with a collapsibility index of $<30\%$, who had a decrease in right ventricular outflow velocities only to 30%. Fluid challenge reduced the variation in superior vena caval diameter through a change in caval zone condition in a similar fashion to the West zones conditions (Fig. 9.7).

Several Doppler indices have been studied to estimate left ventricular filling pressure. These are provided through pulsed-wave (PW) Doppler interrogation of the MV inflow, the pulmonary venous flow (PVF) (Fig. 9.8) and more recently, the use of tissue Doppler interrogation of the MV annulus. Acute preload reduction is associated with a reduction of the E/A ratio on the MV inflow signal: this pattern has been shown to correlate with left ventricular filling pressure in several studies (13,14). Not only is the E/A ratio related to pulmonary capillary wedge pressure (PCWP) (15), but the difference between the duration of the atrial reversal wave in the pulmonary veins and that of the mitral A-wave is a useful variable for the estimation of LVEDP (16). As downstream left ventricular filling pressure is increased, the duration of the atrial reversal in the pulmonary veins increases and exceeds the duration of the mitral A-wave. The PVF flow pattern has also been studied as an index of preload. Kuecherer et al. (17) reported the inverse relationship between the PVF ratio of the systolic to diastolic (S/D) velocity–time integral and the left atrial filling pressure (17). Girard et al. (18) demonstrated a greater respiratory variation of the systolic component (S) with PCWP <18 mmHg (18). Lattik et al. (19) observed that patients with normal or mildly abnormal diastolic function and a low to normal E/A ratio respond to a fluid bolus by increasing their CO and SV as opposed to patients with elevated E/A ratio (Fig. 9.9). The MV E/A ratio was superior to left ventricular filling pressure and 2D echocardiographic area measurements in predicting the response to volume infusion (19).

More recently, the velocity of propagation (V_p) of the E-wave assessed by color M-mode and tissue Doppler imaging of the MV annulus have been used in the estimation of LV filling pressure. The E/e ratio of the MV

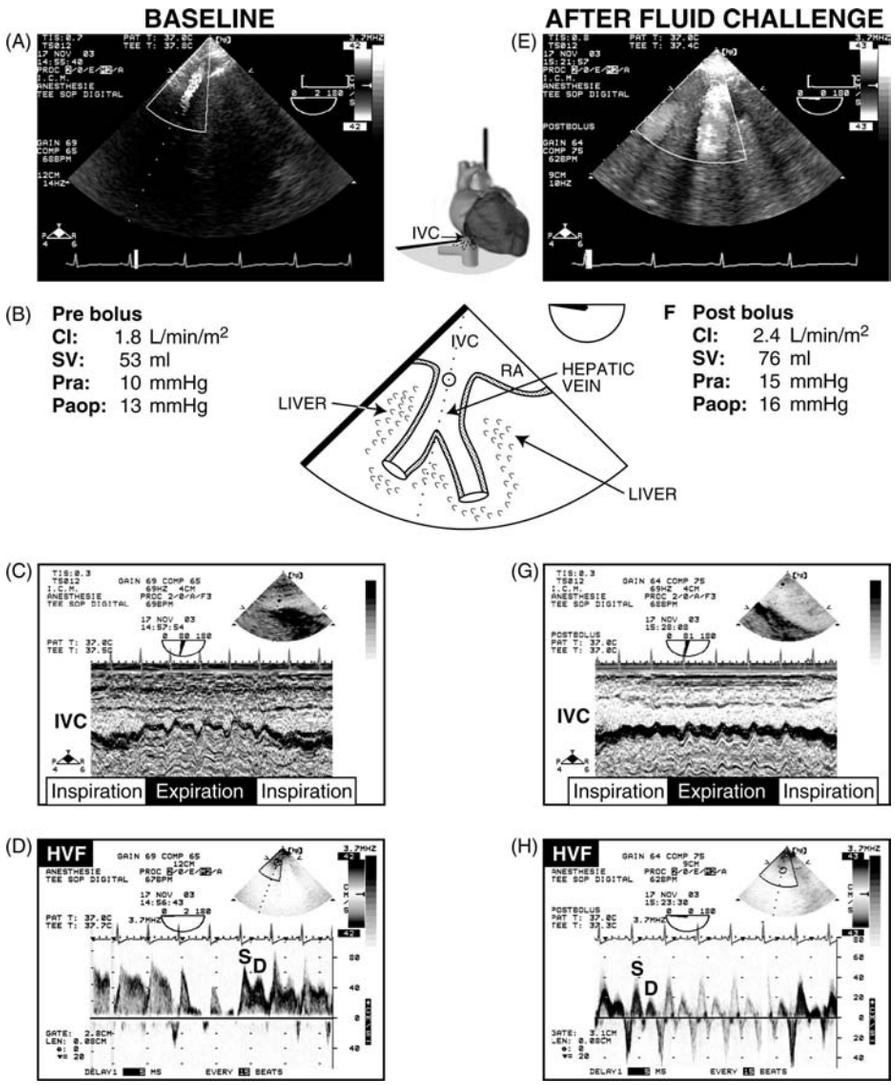

Figure 9.7 Effect of fluid loading on hemodynamic and echocardiographic parameters in a 62-year-old man on mechanical ventilation. (A–D) Baseline: the diameter of the inferior vena cava (IVC) and hepatic veins is small. (C) The IVC collapse during the lowest intrathoracic pressure period: here with the expiration phase of positive-pressure ventilation. (D) Hepatic venous flow (HVF) Doppler interrogation: systolic velocities are elevated up to 80 cm/sec because of the small hepatic vein caliber. (E–H) After fluid challenge, the diameter of the IVC and hepatic veins has enlarged. (F) The cardiac index (CI) and filling pressure increased. (G) Significant IVC collapse is absent. (H) The larger diameter of the hepatic vein results in lower velocities (Paop, pulmonary artery occlusion pressure; Pra, right atrial pressure; RA, right atrium; SV, stroke volume).

inflow E velocity to the MV annulus e (also labeled E_m) ≥ 9 best identifies patient with LVEDP >12 mmHg (20,21). Likewise, the E/V_p ratio of the MV inflow E velocity to the color M-mode V_p with a value >1.5 best identified patients with PCWP >12 mmHg (22,23). Both E/e and E/V_p ratios have been shown to correlate well with left ventricular filling pressure independently of ventricular function. Table 9.1 summarizes the effect of a reduction or an increase in preload on these Doppler parameters.

2. *Afterload*

An increase in afterload will be associated with an increase in the LVESP necessary to open the AoV and consequently the LVESV will increase [Fig. 9.4(B)], while the slope of the relationship or the elastance remains unchanged. In the preoperative clinical setting, we do not routinely measure echocardiographic indices of afterload. It can however be estimated using the arterial

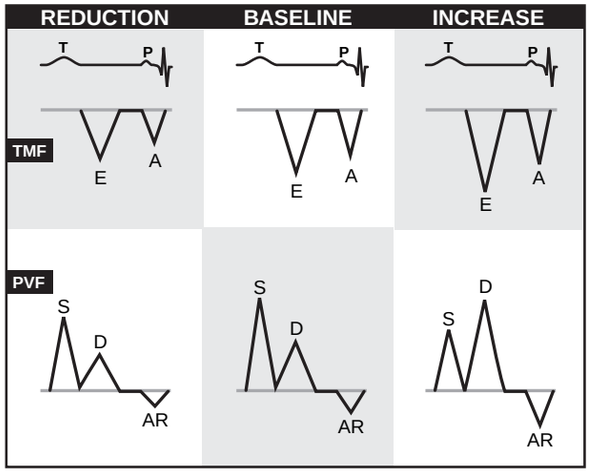

Figure 9.8 Effect of changes in preload on the pulsed-wave Doppler interrogation of the transmitral valve flow (TMF) and the pulmonary venous flow (PVF). With reduction in volume, both the early diastolic mitral valve inflow E-wave and the diastolic D-wave of the PVF are reduced. With increase in preload, the TMF E-wave and PVF D-wave are increased (AR, atrial reversal).

elastance, that is, the ratio of LVESP over the LVESV (24) or by estimating the LVES wall stress which combines M-mode or 2D measurements with pressure data (see Chapter 5). An often unrecognized important clinical scenario leading to an increase in afterload is seen with the systolic anterior motion (SAM) of the MV and its associated left ventricular outflow tract (LVOT) obstruction which results in mosaic flow due to aliasing on color imaging of the LVOT (Fig. 9.10). Systolic anterior motion of the MV can occur during MV repair and several other extreme physiologic situations during which left ventricular filling is significantly reduced.

3. Contractility and Ventricular Performance

Changes in preload and afterload will displace the pressure–volume loops along a line called maximal elastance. Decreasing or increasing contractility will be associated with a downward or upward shift of the elastance and a displacement of the pressure volume relationship towards the right. In Fig. 9.4(C), for instance, the decrease in contractility (dotted loop) results in a greater LVESV for the same LVESP. The concept of elastance is important to understand because this measure is considered relatively independent of changes in preload and afterload. Measurements such as ejection fraction and CO are not pure indices of contractility but rather markers of ventricular performance. Consequently, changes in preload or afterload may affect the ejection fraction but no changes in elastance will be observed. A study with

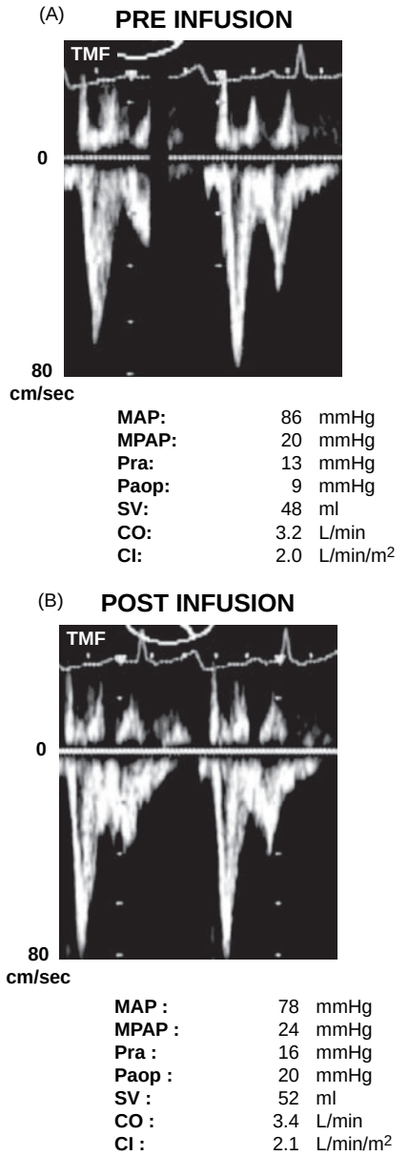

Figure 9.9 Echocardiographic and hemodynamic effect of volume loading: a high baseline E/A ratio predicts limited response to fluid infusion. (A) The transmitral flow (TMF) early diastolic E-wave is predominant compared with the atrial A-wave. (B) Following a bolus of 500 mL of a colloid solution, the E/A ratio increased. This was associated with an increase in mean pulmonary artery pressure (MPAP), right atrial pressure (Pra), pulmonary artery occlusion (Paop) or "wedge" pressure but no significant change in mean arterial pressure (MAP), stroke volume (SV), cardiac output (CO), and cardiac index (CI).

patients undergoing coronary artery bypass also documented the fact that despite the absence of significant postoperative change in SV, fractional area change (FAC) and CO, the elastance index suggested a reduction in

Table 9.1 Summary of the Doppler Indices in the Evaluation of Hypovolemia

	Decrease in filling pressure	Increase in filling pressure
MV inflow PW Doppler		
E velocity	↓	↑
A velocity	↑	↓
E/*A* ratio	↓	↑
Deceleration time	↑	↓
Pulmonary veins PW Doppler		
S velocity	↑	↓
D velocity	↓	↑
AR velocity	↓	↑
AR duration	↓	↑
S/*D* TVI ratio	↑	↓
Respiratory variations	↑	↓
MV annulus tissue Doppler		
e velocity	↑	↓
Color M-mode		
Velocity of propagation (V_p) of the E-wave	↑	↓
Derived indices		
Difference A wave duration (MV–PV)	↓	↑
E/*e*	↓	↑
E/V_p	↓	↑

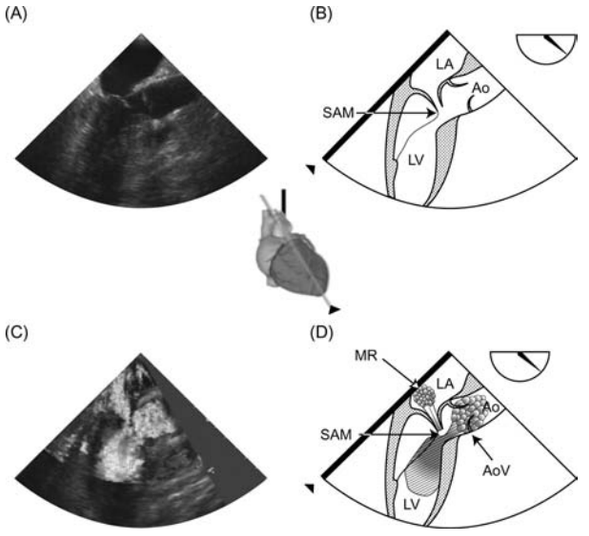

Figure 9.10 Dynamic left ventricular outflow tract obstruction: mid-esophageal long-axis view in a 38-year-old man with septic shock and hemodynamic instability. (A, B) Part of the anterior mitral valve is obstructing the left ventricular outflow tract. (C, D) This was associated with mitral regurgitation (MR). His hemodynamic condition improved with fluid and β-blockade (Ao, aorta; AoV, aortic valve; LA, left atrium; LV, left ventricle; SAM, systolic anterior motion).

contractility after the surgical procedure (Fig. 9.11) (25). In clinical practice, elastance is rarely obtained because artificial preload alteration is required to calculate the slope of the pressure–volume relationship.

The most commonly used echocardiographic evaluation of ventricular performance includes measurements of FAC, ejection fraction and CO. Fractional area change provides an estimation of ejection fraction and is commonly obtained from a transgastric view (Fig. 9.5). Ejection fraction calculation can be obtained through the measurement of ventricular volumes from the four- and two-chamber views using one of several formulas available for volume measurements (see Chapter 5) (2). Stroke volume and secondly CO can be calculated from either 2D volume end-diastolic and end-systolic measurements, or from volumetric Doppler-derived results (see Chapter 5). Other indirect echocardiographic signs useful in the identification of reduced left ventricular systolic function include the presence of intracavitary spontaneous echo contrast, increased anterior MV leaflet septal distance (see Fig. 10.22) reduced mitral annular displacement (26) and an abnormal myocardial performance index (27). The latter (see Fig. 9.12) is altered by abnormalities in either systolic and/or diastolic function and it can be used in the evaluation of both left and right ventricular function (28,29).

III. ABNORMAL LEFT VENTRICULAR FUNCTION

A. Acute vs Chronic Etiology

Acute left ventricular dysfunction can be either systolic or diastolic in origin. It is typically associated with both increased wall motion score index (see Chapter 8) and moderate to severe diastolic dysfunction. Severe left ventricular systolic dysfunction will sometimes be accompanied by pulsus alternans, where the left ventricular stroke volume and systolic blood pressure will be decreased on every alternate beat (Fig. 9.13). Left ventricular diastolic dysfunction is commonly seen in unstable patients after cardiac surgery, even in patients with normal systolic function (30). Chronic left ventricular systolic dysfunction will be associated with ventricular dilatation and diastolic dysfunction which severity can range from mild delayed relaxation to restrictive filling pattern (see following text). Atrial dilatation is more common in chronic condition but can be observed also in the acute setting and often correlates with the degree of diastolic dysfunction. This can be associated with mitral annular dilatation, mitral regurgitation (MR), and atrial fibrillation.

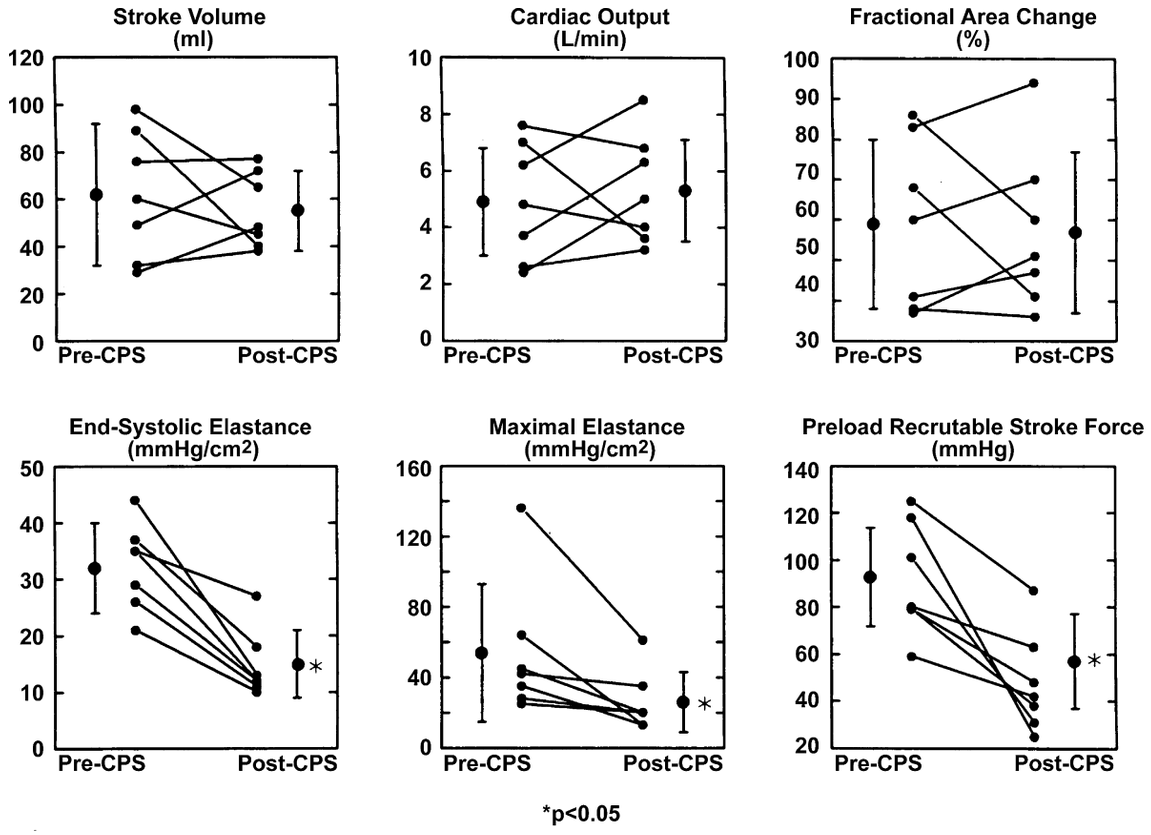

Figure 9.11 Changes in stroke volume, cardiac output, fractional area change, end-systolic elastance, maximal elastance, and preload recruitable stroke force in seven patients before and after cardiopulmonary bypass surgery (CPS). No significant changes were observed in stroke volume, cardiac output and fractional area change. However the indices based on the pressure–volume relationship were lower after CPS. [With permission of Gorcsan et al. (25).]

B. Problems Confounding Diagnosis

In the evaluation of left ventricular function, several errors can be made in the measurement of left ventricular dimensions. In the mid-esophageal four-chamber view, the apex of the LV can be foreshortened leading to underestimation of ventricular volume. Further retroflexion of the probe tip may reduce the impact of this problem. A transgastric short-axis view with an oblique cross section leads not only to faulty measurements of left ventricular dimensions, but also to misinterpretation of regional wall motion. Moderate to severe MR or ventricular septal defect may result in a left ventricular ejection fraction which overestimates intrinsic myocardial contractility. The presence of MR allows the measurement of left ventricular dP/dt, a different index of left ventricular contractility and function (Fig. 9.14) which can be used to estimate ejection fraction postoperatively (31). Finally, the estimation of left ventricular ejection fraction may vary according to the site of measurement as one moves from the ventricular apex (75%) to the short axis (65%) to the base of the heart (50%). Longitudinal contraction (shortening of the left ventricle long axis) contributes 10–15% of the ejection fraction.

C. Transesophageal Echocardiographic Evaluation

Figures 9.15–9.18 summarize our approach to the evaluation of ventricular function using four specific views that allow the evaluation of both left and right ventricular systolic and diastolic dysfunction and also mitral, aortic, and tricuspid valvular function.

IV. ABNORMAL RIGHT VENTRICULAR FUNCTION

A. Importance

Right ventricular systolic dysfunction is associated with high morbidity after cardiac surgery (32,33), chest trauma (34) and with sepsis (35) and can be difficult to diagnose

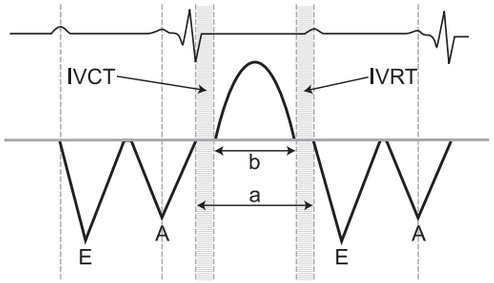

$$a = IVRT + IVCT + ET$$

$$b = ET$$

$$MPI = \frac{a - b}{b} = \frac{IVRT + IVCT}{ET}$$

Normal value: LV = 0.39 ± 0.05
RV = 0.28 ± 0.04

Figure 9.12 Measurement of myocardial performance index (MPI) or Tei index. (1) For the MPI of the left ventricle (LV), the transmitral inflow is used for measurement of the duration "a" from the end of atrial contraction (A-wave) to the beginning of LV filling (E-wave). (2) The ejection time (ET) or "b" is measured from a deep transgastric long-axis view Doppler interrogation of the left ventricular outflow tract. The MPI of the right ventricle (RV) is similarly obtained using the transtricuspid flow and the mid-esophageal ascending aorta short-axis view for the right ventricular outflow tract (IVCT, isovolumic contraction time; IVRT, isovolumic relaxation time) (28).

with conventional hemodynamic criteria after cardiac surgery (30). Davila-Roman et al. (36) observed that right ventricular dysfunction cannot be differentiated from left ventricular dysfunction using pulmonary artery catheter-derived variables in the postbypass period. This stresses the importance of the echocardiographic assessment of right ventricular function. The RV is anterior to the LV and has a crescentic configuration. Because of this complex shape, which is more difficult to describe by a mathematical geometric model, right ventricular volume has been more difficult to estimate from 2D parameters compared with the left-sided volume.

B. Transesophageal Echocardiography Findings

Echocardiographic evaluation of right ventricular function includes measurements of chamber size, evaluation of regional wall motion, ventricular septal motion, tricuspid annular displacement, and vena cava size. Evaluation can be complemented with PW Doppler interrogation of the pulmonary outflow tract, tricuspid inflow and hepatic venous flow and tissue Doppler interrogation of the tricuspid annulus. These measurements can be obtained using the four-chamber view (Fig. 9.15), the transgastric short- (Fig. 9.17) and long-axis view (Fig. 9.18) of the RV. Echocardiographic manifestations of right ventricular failure

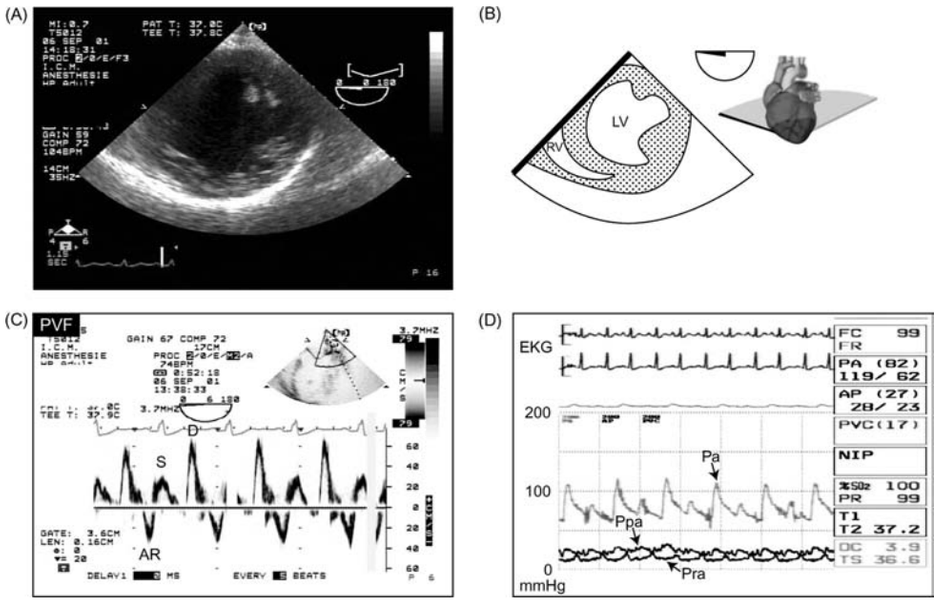

Figure 9.13 Left ventricular severe systolic and diastolic dysfunction in a 71-year-old woman before revascularisation. (A, B) The mid-papillary transgastric short-axis view demonstrates dilated left ventricle (LV) with severe systolic dysfunction. (C) Pulmonary venous flow (PVF) showing diastolic predominance ($S < D$) consistent with moderate diastolic dysfunction. (D) Pulsus alternans on the arterial pressure (Pa) tracing was present (AR, atrial reversal; EKG, electrocardiogram; Ppa, pulmonary artery pressure; Pra, right atrial pressure; RV, right ventricle).

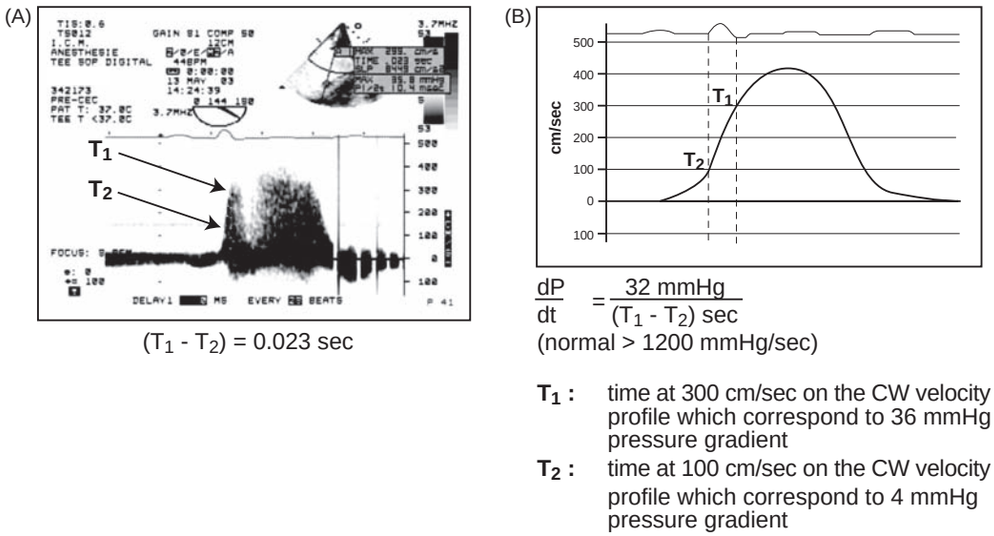

Figure 9.14 Measurement of left ventricular change in pressure over time (dP/dt) using continuous-wave Doppler of mitral regurgitation in a 58-year-old man. Before surgery the left ventricular dP/dt was 32 mmHg per 0.023 s = 1391 mmHg/s.

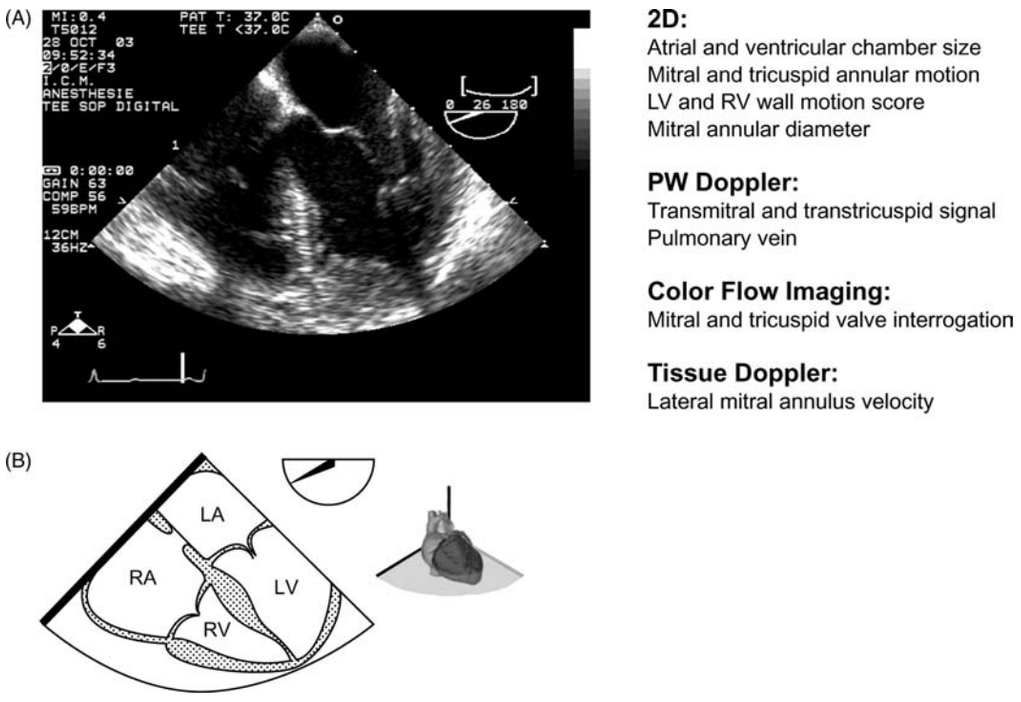

Figure 9.15 Biventricular function evaluation. Using a mid-esophageal four-chamber view, right and left atrial and ventricular dimensions are evaluated as well as regional contractility and mitral annular motion. Volumetric stroke volume through the mitral valve is measured with the mitral annulus diameter and modal time-velocity integral of pulsed-wave Doppler of mitral inflow at the annulus level. Both the transmitral and transtricuspid pulsed-wave Doppler inflow signal correct alignment for Doppler measurement should be verified by color flow imaging. The lateral mitral annular plane is evaluated with tissue Doppler and with left-sided rotation and pull-back. The left upper pulmonary vein can also be interrogated (LA, left atrium; LV, left ventricle; RA, right atrium; RV, right ventricle).

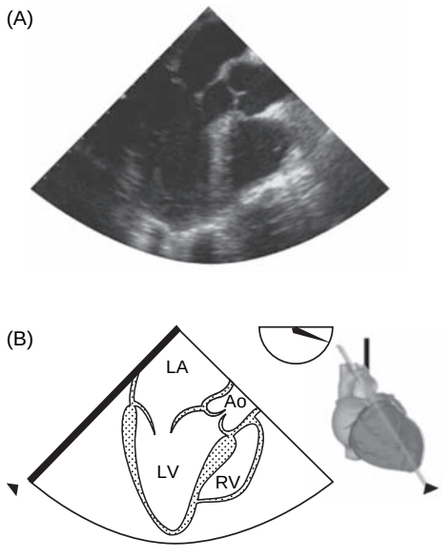

PW Doppler:
Transmitral Doppler signal
IVRT
Transmitral Doppler signal at annulus
(for CO calculation)

Color Flow Imaging:
Mitral and aortic valve interrogation

Tissue Doppler :
Mitral annulus interrogation

Color M-mode:
Mitral inflow Vp measurement

Figure 9.16 Mid-esophageal view at 130° is ideal to quickly screen for both mitral and aortic regurgitation with color Doppler. The transmitral pulsed-wave Doppler signal is often of higher quality than at 0°. Isovolumic relaxation time (IVRT), tissue Doppler interrogation of the mitral annulus and color M-mode velocity of propagation (*V*p) are easily obtained. Cardiac output (CO) of the left ventricle (LV) can be obtained using mitral annulus diameter and pulsed-wave (PW) Doppler interrogation of the mitral valve at the same level (Ao, aorta; LA, left atrium; RV, right ventricle).

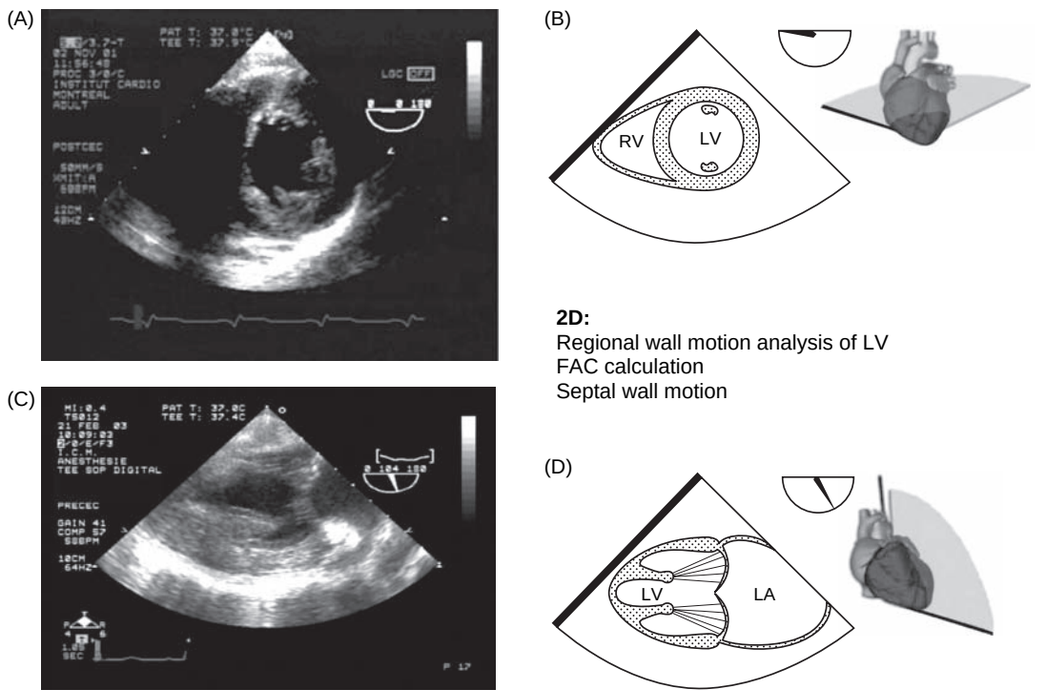

2D:
Regional wall motion analysis of LV
FAC calculation
Septal wall motion

Figure 9.17 Evaluation of systolic function of the left ventricle (LV). (A, B) The mid-papillary short-axis view is obtained for the fractional area change (FAC) calculation and wall motion score of the LV. Attention is paid to septal wall motion which can be altered with right ventricular dysfunction. (C, D) A 90° view is obtained to ensure that the mid-papillary view is perpendicular to the ventricular axis and to complete the basal and apical wall motion score evaluation of the four-chamber (LA, left atrium; RV, right ventricle).

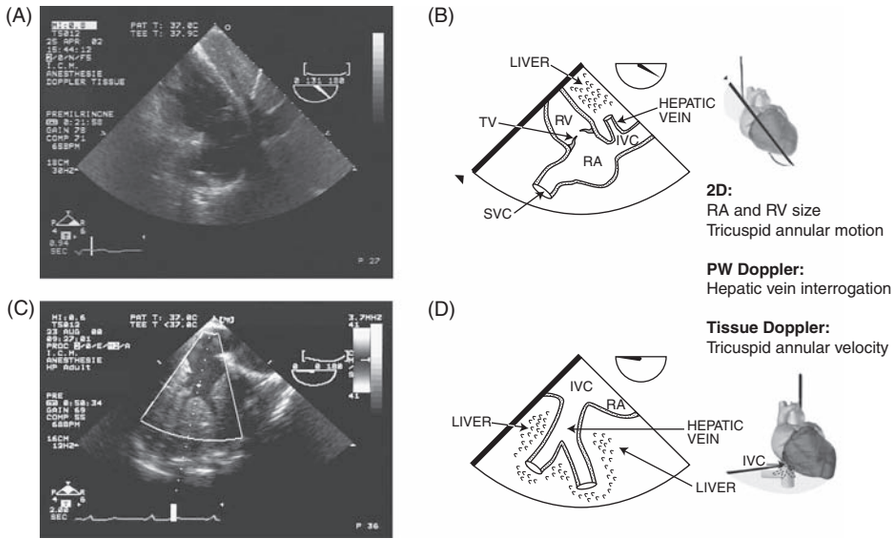

Figure 9.18 Evaluation of systolic and diastolic function of the right ventricle (RV). (A, B) Transgastric right ventricular long axis. Right chamber size is evaluated. Pulsed-wave (PW) Doppler interrogation of the hepatic vein and tissue Doppler evaluation of the tricuspid annulus. (C, D) Alternative deep esophageal 0° position with rightward rotation to perform PW Doppler interrogation of the hepatic vein (IVC, inferior vena cava; RA, right atrium; SVC, superior vena cava; TV, tricuspid valve).

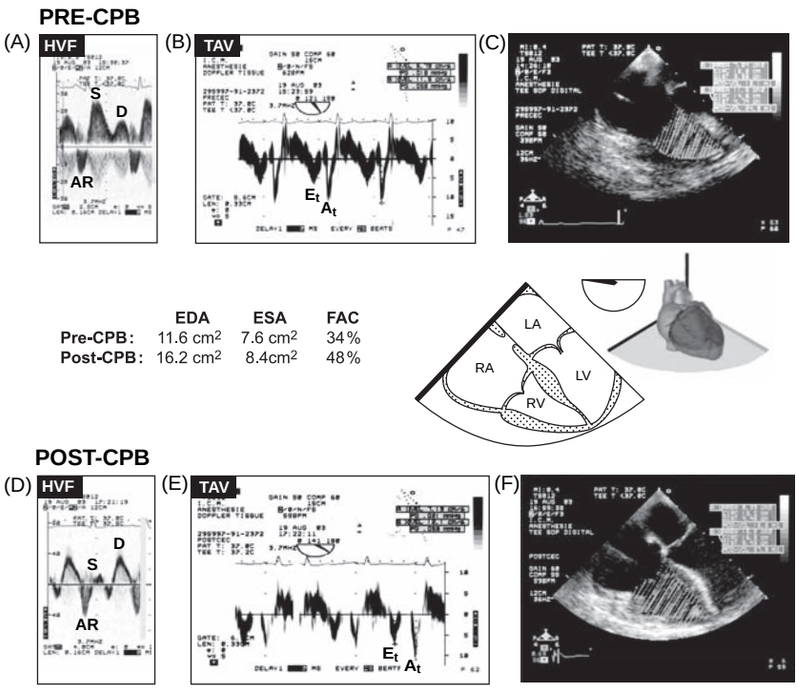

Figure 9.19 Systolic and diastolic function of the right ventricle (RV) in a 65-year-old man with previous inferior myocardial infarction scheduled for coronary revascularization. (A–C) Before cardiopulmonary bypass (CPB): the ejection fraction of the left ventricle (LV) is 20% with a low cardiac index of 1.5 L/min per m^2. (A) Pulsed-wave Doppler hepatic venous flow (HVF) shows systolic flow S predominance. (B) Tissue Doppler of tricuspid annular velocities (TAV) shows a E_t/A_t ratio <1 ($E_t = 5.7$ and $A_t = 11.5$ cm/sec). Both suggest mild diastolic dysfunction of the RV. (C) The fractional area change (FAC) of the RV is 34%. (D–F) Post-CPB. (D) The HVF showed new blunting of the systolic flow S. (E) The TAV are increased with a similar ratio ($E_t = 7.1$ and $A_t = 12.1$ cm/sec). This suggests decreased RV compliance. (F) Right ventricular FAC increased to 48% consistent with the surgeon's visual appreciation of improved right ventricular function. Upon arrival to the intensive care unit, the cardiac index was 3.0 L/min per m^2 (AR, atrial reversal; EDA, end-diastolic area; ESA, end-systolic area; LA, left atrium; RA, right atrium).

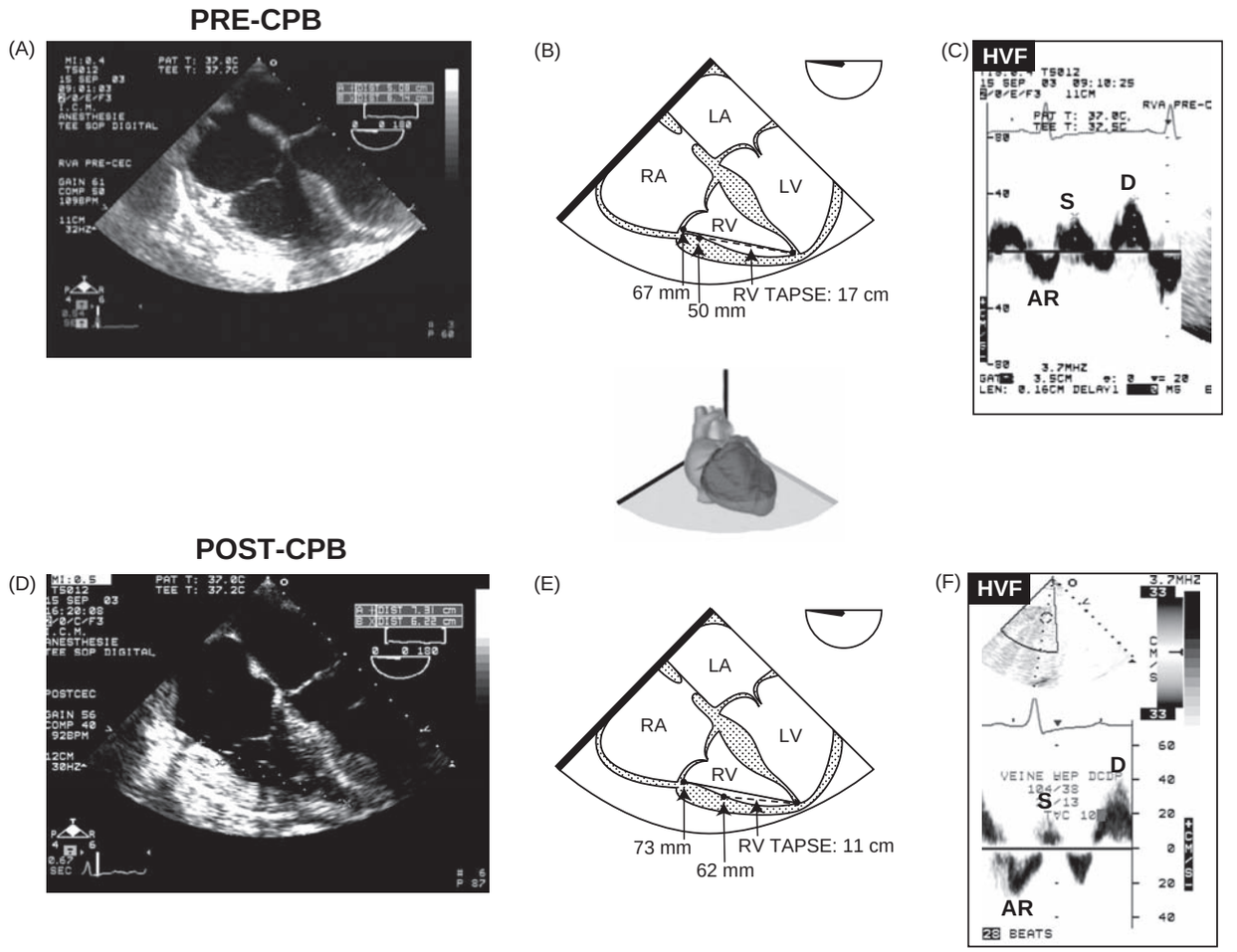

Figure 9.20 Evaluation of right ventricular systolic function. (A, B) Tricuspid annular plane systolic excursion (TAPSE) was 17 mm/67 mm (25%) before cardiopulmonary bypass (CPB). (C) Hepatic venous flow (HVF) was abnormal before CPB with systolic attenuation. (D, E) After CPB, TAPSE was 11 mm/73 mm (15%). (F) Systolic attenuation was more pronounced post-CPB (AR, atrial reversal; LA, left atrium; LV, left ventricle; RA, right atrium; RV, right ventricle; TV, tricuspid valve).

are RV and RA dilatation, reverse convexity of the atrial septum towards the LA, right to left shunting through a patent foramen ovale, reduction in annular tricuspid displacement (37), and abnormal Doppler profile of the hepatic veins (38,39). Right ventricular dilatation is considered mild, moderate, or severe when the RVEDA measured from a four-chamber view is smaller, equal or greater than LVEDA. The right ventricular area, calculation of right ventricular FAC (Fig. 9.19) and tricuspid annular motion (Fig. 9.20) (40) can be obtained using a four-chamber view (33). With right ventricular volume overload, the RV will be dilated and the ventricular septum, normally convex towards the RV, will be flattened or even convex towards the LV during diastole only (Fig. 9.21), with associated paradoxical motion during systole. With right ventricular pressure overload, flattening of the ventricular septum occurs during both systole and diastole.

V. ABNORMAL DIASTOLIC FUNCTION

A. Left Ventricular Diastolic Dysfunction

Diastolic function should be an integral part of the evaluation of cardiac function. Indeed, left ventricular diastolic dysfunction is a predictor of difficult weaning from bypass as good as systolic dysfunction (41). Diastolic dysfunction can be isolated or associated with systolic dysfunction or pericardial disease. Echocardiographically, left ventricular diastolic dysfunction has been classified as mild (impaired left ventricular relaxation), moderate (pseudonormal pattern) and severe (left ventricular restrictive filling) with increasing left ventricular filling pressures. We use a combination of Doppler-derived variables in the diagnosis of left ventricular diastolic dysfunction (Fig. 9.22) and a diagnostic algorithm (Fig. 9.23) (42).

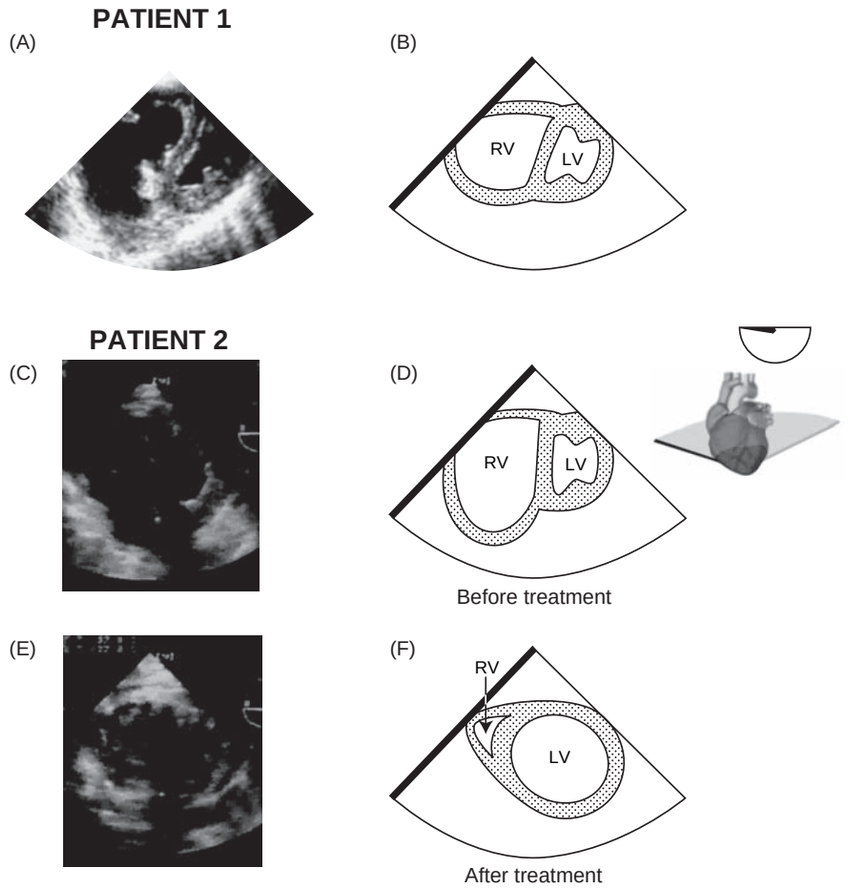

Figure 9.21 Systolic dysfunction of the right ventricle (RV) in two different patients. (A, B) Transgastric view of a 50-year-old woman with severe pulmonary hypertension associated with scleroderma. The RV is dilated with a D-shaped left ventricle (LV) and systolic septal flattening. (C–F) Right ventricular dysfunction from fluid overload in another patient before (C, D) and after (E, F) vasodilator therapy. Note the reduction in right ventricular size and change in septal curvature after treatment.

Diastolic dysfunction alters the pressure volume relationship [Figs. 9.4(D–F)] and could explain some of the observed changes in this relationship between filling pressure and ventricular volume observed after cardiopulmonary bypass (CPB) (Fig. 9.3). Impaired or delayed relaxation (mild diastolic dysfunction) results in decreased left ventricular pressure decay during diastole and prolonged isovolumic relaxation time (IVRT). This will be reflected with higher diastolic filling pressure for the same left ventricular volume [Fig. 9.4(D)]. Echocardiographic evaluation of abnormal relaxation using PW Doppler interrogation of the MV will demonstrate prolonged IVRT, prolonged E-wave deceleration time, and a reduction of the E/A ratio. The pulmonary vein PW Doppler signal will show an increased S/D ratio. Tissue Doppler of the mitral annulus will demonstrate an E_m/A_m ratio <1 while on color M-mode, V_p will be decreased (Fig. 9.24). The delayed relaxation abnormality is the most common form of diastolic dysfunction (70% in our practice) and is the most sensitive manifestation of myocardial ischemia. It is commonly associated with left ventricular hypertrophy either due to hypertension or aortic stenosis (AS).

Left ventricular restrictive filling abnormality represents a more severe degree of diastolic dysfunction. This is associated with an upward shift of the diastolic pressure–volume curve [Fig. 9.4(F)]. In these patients the following echocardiographic findings are observed: PW Doppler of the mitral inflow reveals shortened IVRT and E-wave deceleration time, a high E/A ratio >2; PW Doppler interrogation of the pulmonary vein shows predominant diastolic flow while tissue Doppler imaging of the mitral annulus demonstrates reduced E_m velocity, and color M-mode propagation velocity will be decreased. This type of abnormality is commonly seen in hemodynamically unstable patients before or after cardiac surgery (Fig. 9.25).

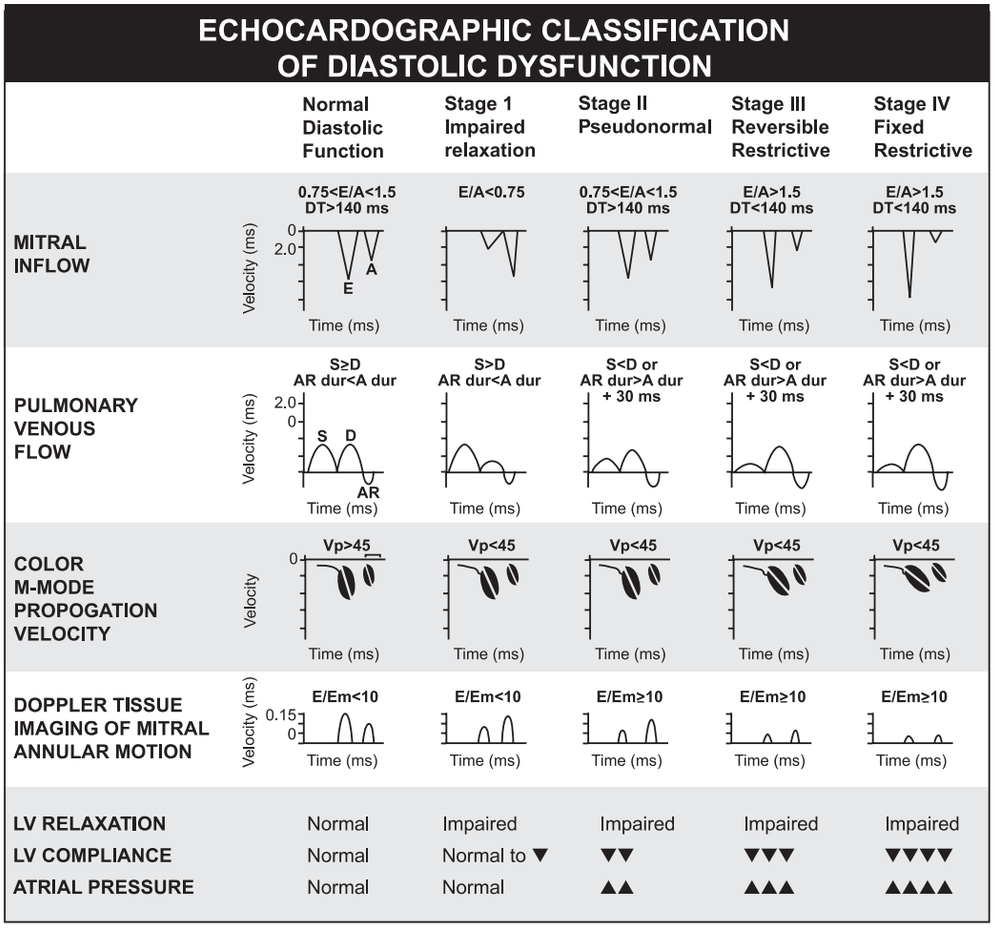

Figure 9.22 Echocardiographic classification of diastolic dysfunction adapted for transesophageal echocardiography (A, peak late diastolic transmitral flow velocity; A dur, duration of mitral inflow A-wave; AR dur, peak pulmonary venous atrial reversal flow velocity duration; D, peak diastolic pulmonary venous flow velocity; DT, deceleration time; E, peak early diastolic transmitral flow velocity; Em, peak early diastolic myocardial velocity; LV, left ventricular; S, peak systolic pulmonary venous flow velocity; V_p, flow propagation velocity). Adapted for TEE. [With permission of Khouri et al. (42).]

Finally, in patients with relaxation abnormalities and increased filling pressure, a moderate or intermediate form of diastolic dysfunction called the pseudonormal pattern is seen. The expression pseudonormal is a consequence of the normal looking PW Doppler mitral inflow signal while the PVF pattern is clearly abnormal ($S/D < 1$). With a pseudonormal pattern, the pressure–volume diagram will demonstrate moderate upward elevation of the diastolic waveform [Fig. 9.4(E)]. Echocardiographically, it is characterized by reduced IVRT, a "pseudo" normal E/A ratio and deceleration time, PVF with inverted S/D ratio <1 and atrial reversal wave velocity exceeding 40 cm/sec, abnormal tissue Doppler of the mitral annulus with a reduced E_m/A_m ratio and abnormally low color M-mode propagation velocity (Fig. 9.26) (42).

These abnormalities represent a spectrum of disease severity ranging from the milder form of diastolic dysfunction, shown by impaired relaxation abnormalities, to the more severe form such as the restrictive filling pattern. In the perioperative monitoring of cardiac function, particularly in the post-bypass setting, we commonly observe changes in diastolic function irrespective of those in systolic function. Worsening of diastolic function tends to correlate with subsequent deterioration of the hemodynamic function (Fig. 9.26). Diastolic dysfunction can occur in conditions other than those previously described such as the brain–heart syndrome secondary to high-grade subarachnoid hemorrhage (Fig. 9.27).

B. Right Ventricular Diastolic Dysfunction

Right ventricular dysfunction in patients undergoing cardiac surgery is also associated with difficult weaning from CPB bypass and hemodynamic instability (30).

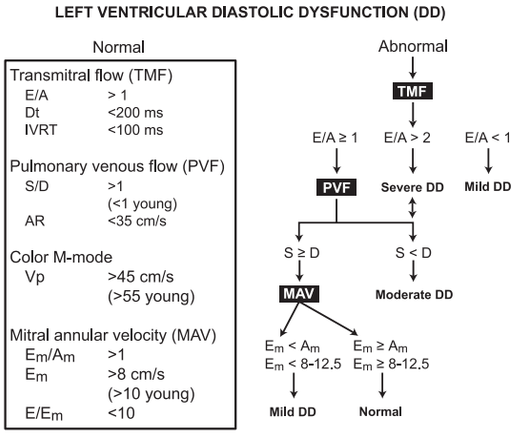

Figure 9.23 Suggested algorithm used in the diagnosis and classification of left ventricular diastolic dysfunction (DD). Diastolic function is classified using pulsed-wave Doppler of transmitral flow (TMF), pulmonary venous flow (PVF) and tissue Doppler examination of mitral annular velocity (MAV). Mild, moderate, and severe DD corresponds to stages I, II, and III. Stage IV corresponds to a fixed restrictive filling pattern. Patients with pacemaker, atrial fibrillation, non-sinus rhythm, moderate to severe mitral regurgitation, those undergoing mitral valve surgery, or with aortic insufficiency are excluded from analysis (AR, atrial reversal; Dt, deceleration time; IVRT, isovolumic relaxation time; V_p, velocity of propagation).

Pulsed-wave Doppler interrogation of the tricuspid valve (TV) inflow (43), hepatic veins (38), and tissue Doppler of the tricuspid annulus (44) (Figs. 9.15 and 9.18) allow assessment of right ventricular diastolic function. An algorithm in the diagnosis of right ventricular diastolic dysfunction is used in our practice (Fig. 9.28). When invasive hemodynamic tracings are available through a pulmonary artery catheter, we have also observed a correlation between the right ventricular diastolic pressure tracing and right ventricular diastolic dysfunction (Figs. 9.29 and 9.30). Examples of right ventricular diastolic dysfunction are shown in Figs. 9.31–9.33. The measurements needed for the evaluation of right ventricular diastolic dysfunction are shown in Figs. 9.15 and 9.18. Using Doppler to evaluate right-sided velocities, it is important to consider the fact that they are associated with a normal 20% respiratory change (see Chapter 13).

VI. CAUSES OF SEVERE HYPOTENSION AND SPECIFIC HEMODYNAMIC DERANGEMENTS

In the hemodynamically unstable patient, Costachescu et al. (30) observed that hypotension may be secondary to several simultaneous factors, all related to problems

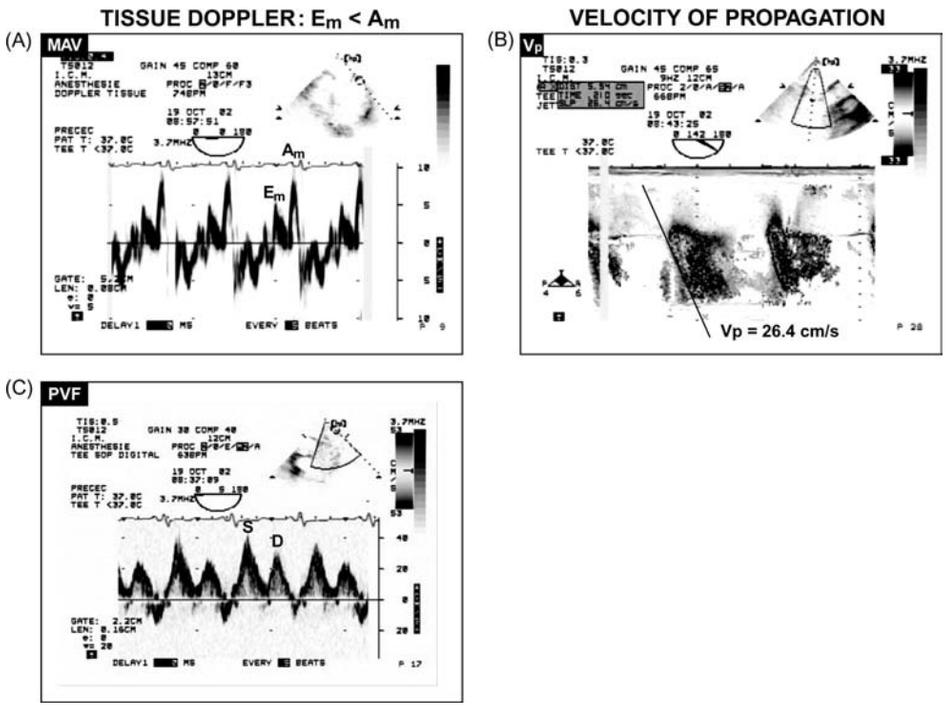

Figure 9.24 Stage 1 diastolic dysfunction (impaired relaxation) in a 72-year-old woman undergoing coronary revascularisation before cardiopulmonary bypass. (A) Tissue Doppler of the lateral mitral annular velocity (MAV): the E_m/A_m ratio is <1. (B) On color M-mode, the propagation velocity (Vp) of the E-wave is 26.4 cm/sec. (C) The pulmonary venous flow (PVF) reveals normal S > D waves.

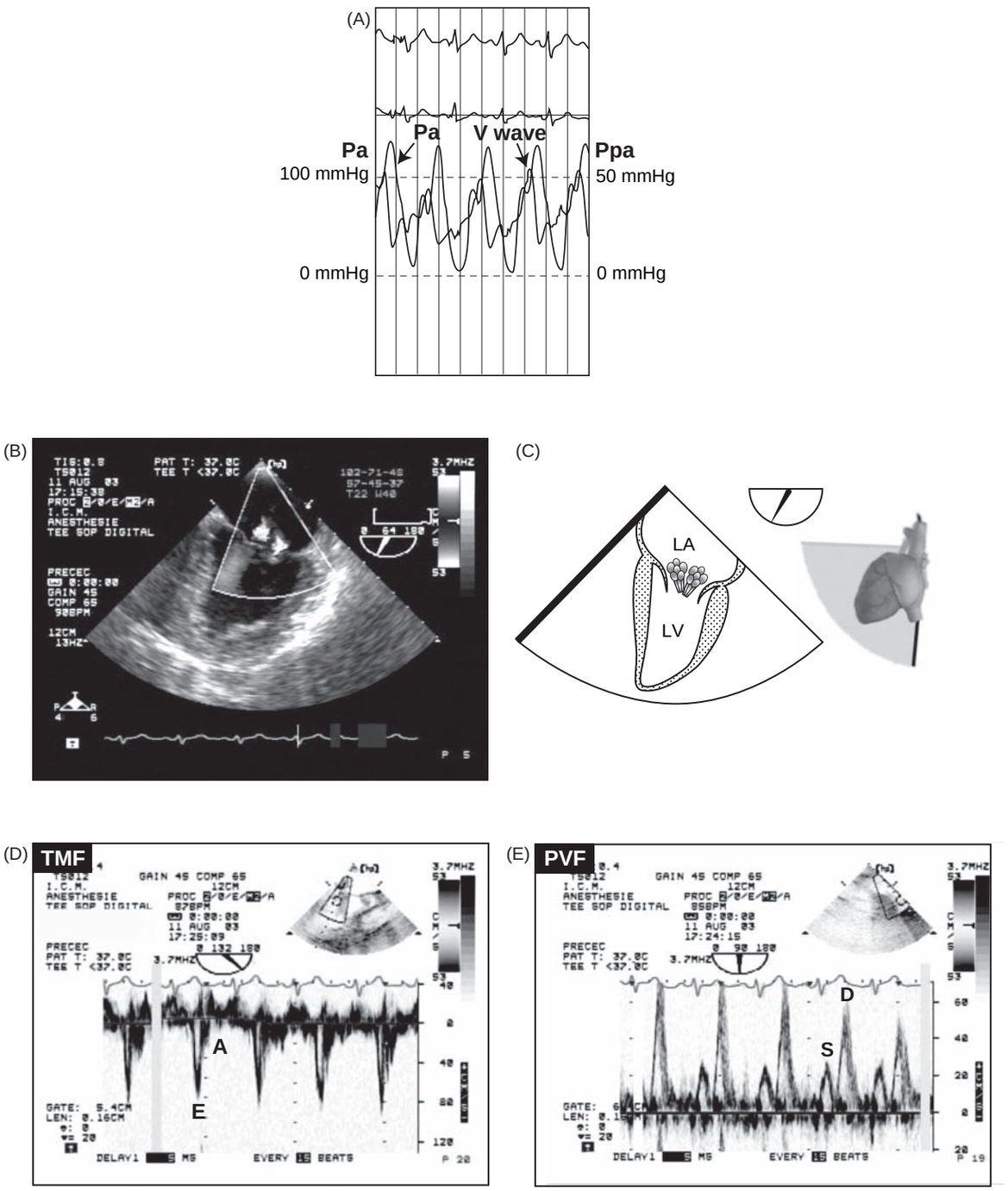

Figure 9.25 Stage III left ventricular diastolic dysfunction (restrictive filling) in a 61-year-old woman with cardiogenic shock brought to the Operating Room for emergency coronary revascularisation. (A) She was hemodynamically unstable on an intra-aortic balloon pump and vasoactive support. A 50 mmHg "V" wave on the wedged pulmonary artery catheter tracing was seen without any significant mitral regurgitation on color flow imaging (B, C). (D) The transmitral flow (TMF) showed an E/A ratio >2 with a deceleration time <60 ms and isovolumic relaxation time of 40 ms. (E) The left upper pulmonary venous flow (PVF) showed an abnormal S/D ratio with S wave blunting (LA, left atrium; LV, left ventricle; Pa, arterial pressure on the 0–100 mmHg left-sided scale, Ppa, pulmonary arterial pressure on the 0–50 mmHg right-sided scale).

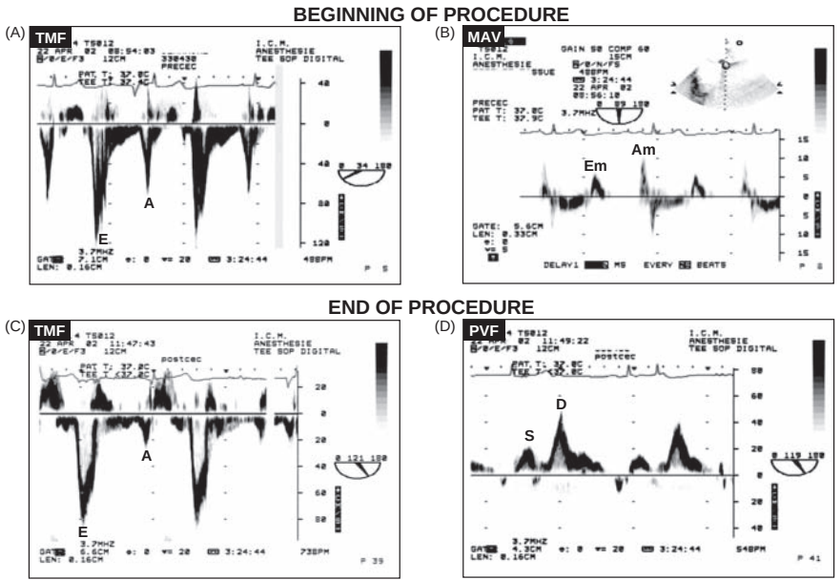

Figure 9.26 Left ventricular diastolic dysfunction in a 73-year-old woman during off-pump bypass surgery. (A, B) At the beginning of the procedure, the transmitral flow (TMF) demonstrates a E/A ratio >1 with a tissue Doppler E_m/A_m ratio <1 (B) consistent with at least moderate diastolic dysfunction (pseudonormal pattern). (C, D) Following revascularization, a higher E/A ratio with left upper pulmonary venous flow (PVF) blunted S-wave suggests worsening diastolic function and higher operating filling pressures. This was associated with significant hemodynamic instability requiring vasoactive support (MAV, mitral annular velocity).

with preload, afterload, contractility and diastolic function rarely acting alone and often in different combinations. Etiologies of hypotension can be grouped according to their mechanism (45). Reduced left ventricular preload can result from hypovolemia, reduced systemic vascular resistance or venous tone, tamponade (see Chapter 11) and decreased right ventricular CO. Increases in left and right ventricular afterload leading to hypotension include left and right ventricular outflow tract obstruction. Reduced contractility and diastolic dysfunction can be

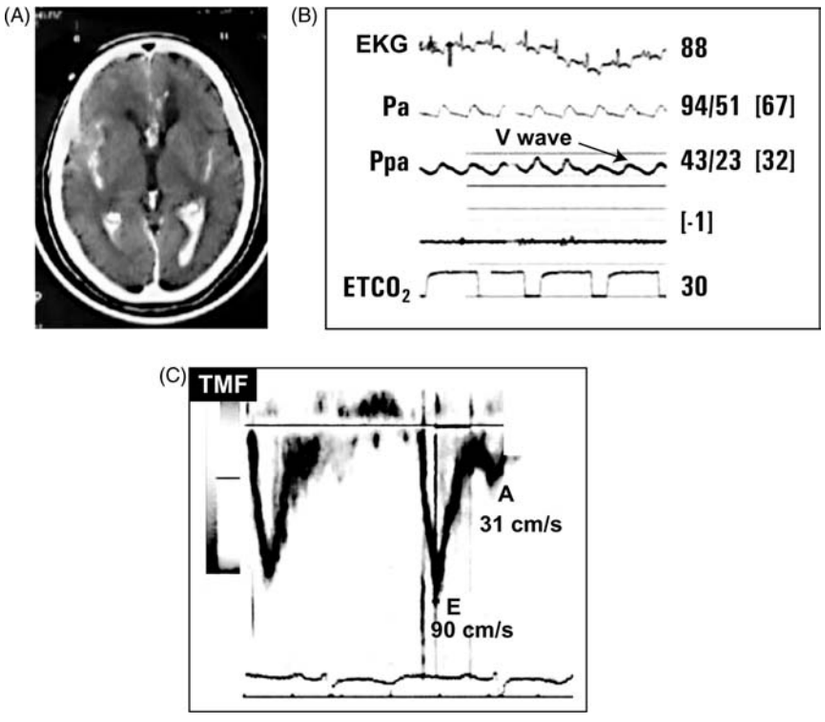

Figure 9.27 Left ventricular diastolic dysfunction in a 37-year-old woman with subarachnoid haemorrhage and brain–heart syndrome associated with hemodynamic instability. (A) The patient's head computed tomography scan showed intraventricular bleeding. (B) The hemodynamic tracing shows a heart rate of 88 beats/min, systolic, and diastolic arterial pressure (Pa) of 94 and 51 mmHg, systolic, and diastolic pulmonary artery pressure (Ppa) of 43 and 23 mmHg with a prominent "V" wave appearing on the wedged tracing without significant mitral regurgitation on color Doppler (not shown). (C) Transmitral flow (TMF) reveals a high E/A ratio (EKG, electrocardiogram; $ETCO_2$, end-tidal carbon dioxide) (Courtesy of Dr. Nancy McLaughlin).

secondary to ischemia. Finally valvular abnormalities (see Chapters 15 and 17) and acquired septal defects (see Chapter 8) are other causes of hypotension. The role of TEE is to assess all potential causes of hypotension and to determine which mechanisms are involved. Some of these conditions will be discussed.

A. Myocardial Ischemia

Myocardial ischemia is the most common cause of hemodynamic instability and is discussed in Chapter 8.

B. Left Ventricular Outflow Tract Obstruction

Left ventricular outflow tract obstruction is a well-known complication of MV repair (46) with or without asymmetric left ventricular hypertrophy (Chapter 10) (47), but is also increasingly recognized in conditions associated with severe preload reduction without significant cardiac disease (Fig. 9.10). The presence of LVOT obstruction has been reported in 5–10% of hemodynamically unstable patients in the intensive care unit (ICU) (48–50). The pressure–volume relationship associated with LVOT obstruction shows the effect of an increased afterload [Fig. 9.4(B)]. In patients with LVOT obstruction, the anterior MV leaflet is displaced into the outflow tract and is associated with MV regurgitation. Distinguishing LVOT obstruction from pure MR as a cause of hemodynamic instability associated with a "v" wave is critical as the treatment of those two conditions is quite different: afterload reduction, inotropic support, and increase in heart rate are recommended for MR but would be deleterious for LVOT obstruction. This abnormality has been observed not only after MV repair but also following AoV replacement (Fig. 9.34). In the operating room (OR) and in the ICU, LVOT obstruction in patients with left ventricular hypertrophy and hypovolemia can also

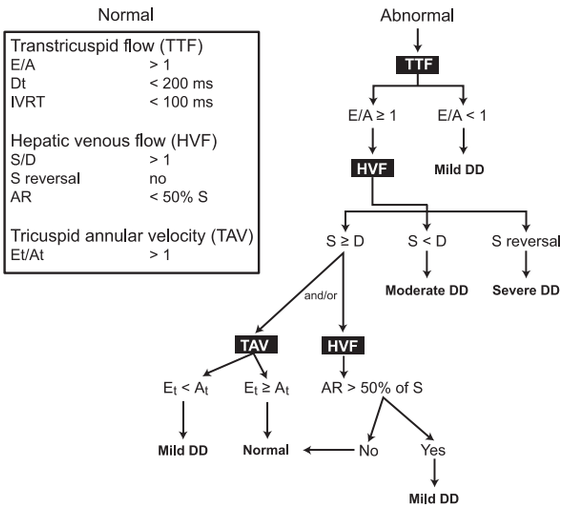

Figure 9.28 Suggested algorithm used in the diagnosis and classification of right ventricular diastolic dysfunction (DD). Diastolic function is classified using pulsed-wave Doppler of transtricuspid flow (TTF), hepatic venous flow (HVF) and tissue Doppler imaging of the tricuspid annulus or tricuspid annular velocity (TAV). Patients with pacemaker, atrial fibrillation, non-sinus rhythm, moderate to severe tricuspid regurgitation, and following tricuspid annuloplasty are excluded from analysis (AR, atrial reversal; Dt, deceleration time; IVRT, isovolumic relaxation time).

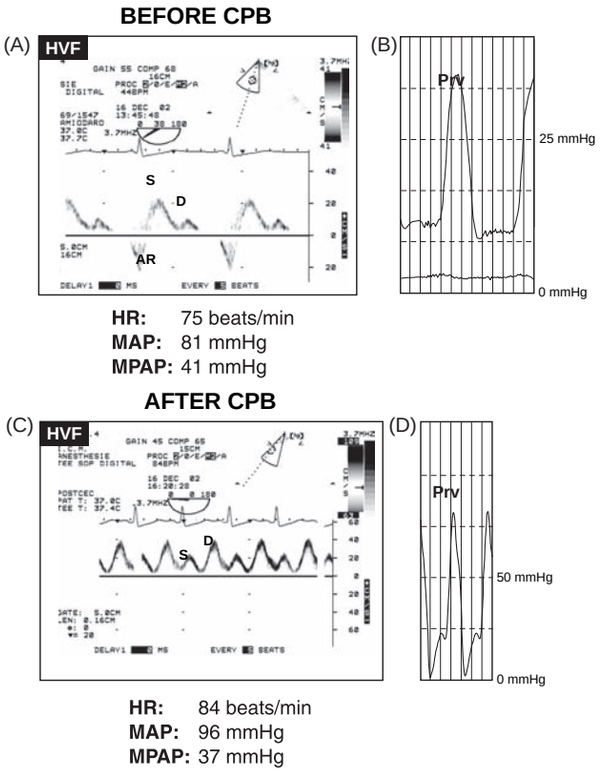

Figure 9.29 Right ventricular diastolic dysfunction in a 56-year-old man who is scheduled for aortic valve replacement. (A) The Doppler hepatic venous flow (HVF) before cardiopulmonary bypass (CPB) showed a normal S/D ratio > 1 but with an increased atrial reversal (AR) wave. (B) He had a normal right ventricular pressure (Prv) waveform despite preoperative pulmonary hypertension with a mean pulmonary artery pressure (MPAP) of 41 mmHg. (C) After CPB, the S/D ratio is <1 with predominant D-wave. (D) This was associated with a change in the slope of the Prv in diastole from a flat to a steep diastolic waveform. Weaning from CPB was difficult requiring 17.5 μg/min of noradrenaline and 0.4 μg/kg per min of nitroglycerine. The abnormal right ventricular filling can be appreciated visually (HR, heart rate; MAP, mean arterial pressure).

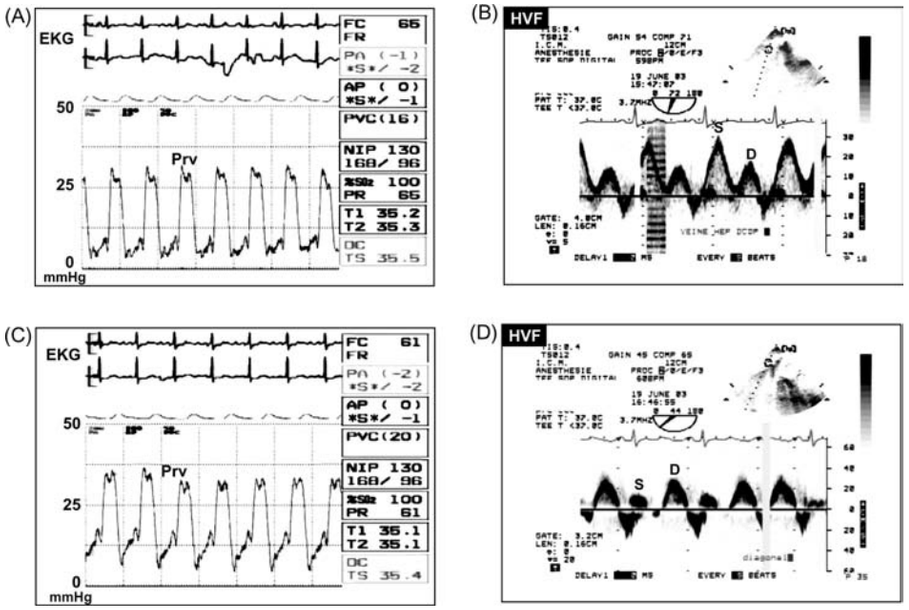

Figure 9.30 Right ventricular diastolic dysfunction during off-pump bypass surgery in a 67-year-old man. (A, B) Baseline: right ventricular pressure (Prv) tracing and hepatic venous flow (HVF) profile. The S/D ratio is >1. (C, D) Hemodynamic instability during clamping of the left diagonal coronary artery. The Prv becomes increasingly steeper in diastole. The S/D ratio is inverted. (EKG, electrocardiogram).

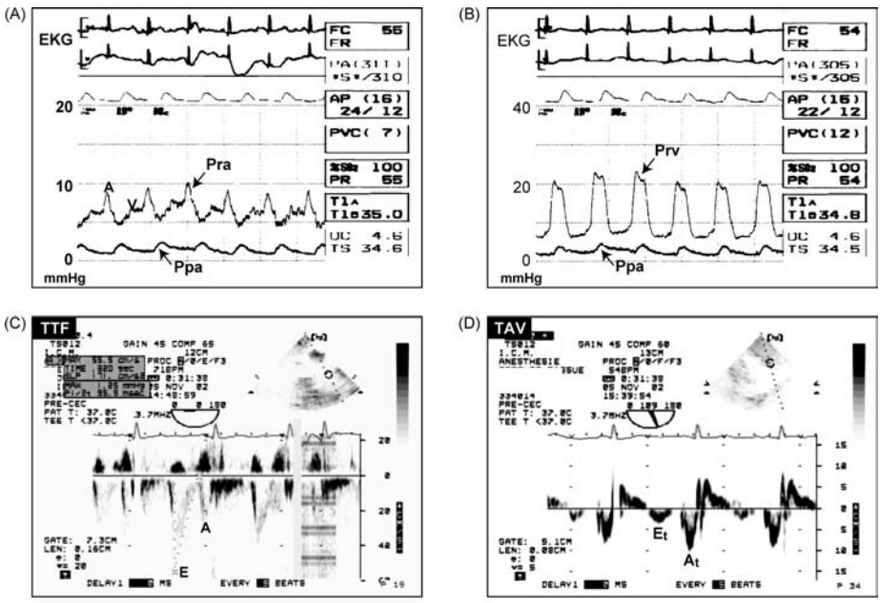

Figure 9.31 Mild right ventricular diastolic dysfunction in a 70-year-old man before cardiac revascularization. (A) On the pressure tracing, the right atrial pressure (Pra) waveform shows a predominant "A" wave. (B) The right ventricular pressure (Prv) tracing shows a normal relatively flat diastolic waveform. (C) The pulsed-wave Doppler transtricuspid flow (TTF) tracing shows a predominant E-wave with a prolonged deceleration time (320 ms). (D) The tricuspid annular velocities (TAV) present an E_t/A_t ratio consistent with mild right ventricular diastolic dysfunction. The hepatic venous flow was normal (not shown). The atrial kick can be seen on the beating heart. The Pra, Prv, and pulmonary artery pressure (Ppa) are on a 0–20, 0–40, and 0–200 mmHg scale respectively (EKG, electrocardiogram).

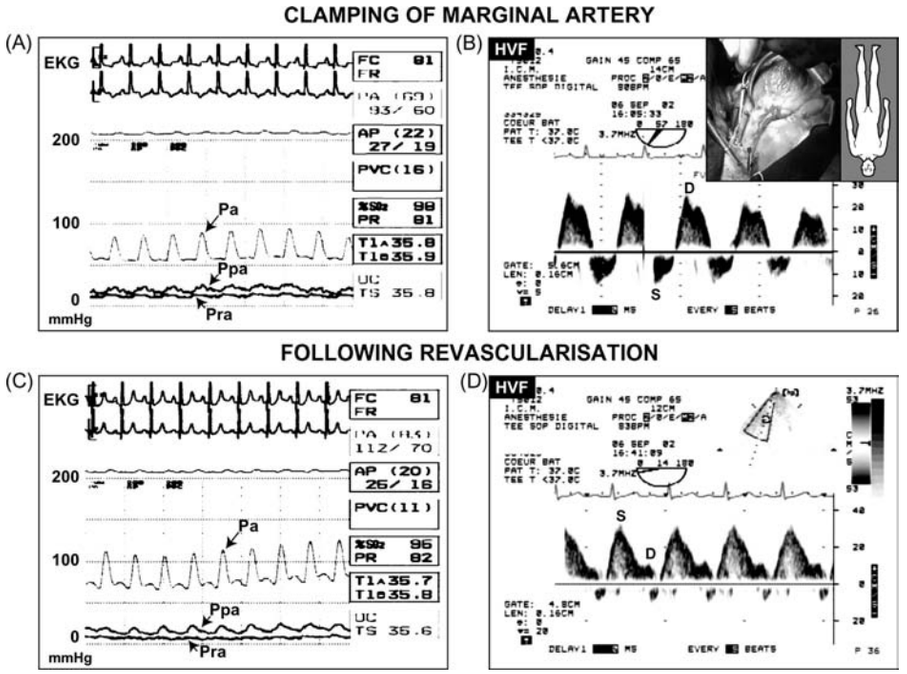

Figure 9.32 Transient severe right ventricular diastolic dysfunction in a 72-year-old patient undergoing off-pump bypass surgery. During clamping of the left obtuse marginal artery, the patient became hemodynamically unstable. (A) This was associated with a reduction in systolic and diastolic systemic arterial blood pressure (Pa) down to 93/60 mmHg, a slight increase in systolic and diastolic pulmonary artery pressure (Ppa) of 27/19 mm Hg and an increase in right atrial pressure (Pra) of 16 mmHg. (B) Systolic flow reversal in the hepatic venous flow (HVF) was present. (C, D) These abnormalities normalized after revascularization was completed. (Photo in B courtesy of Dr. Raymond Cartier).

occur (Fig. 9.10). Left ventricular outflow tract obstruction has also been reported with apical myocardial infarction (51), with the use of intra-aortic balloon counterpulsation (52), with MV prolapse and during lung transplantation (53).

C. Right Ventricular Outflow Tract Obstruction

Right ventricular outflow tract (RVOT) obstruction can be extrinsic or intrinsic. Extrinsic compression can occur for instance from an aortic (54) or pulmonary artery aneurysm (55), mediastinal hematoma (56), or from direct surgical compression during off-pump surgery. Intrinsic compression can be seen in congenital heart disease (57), congenital surgery (58), septal patch repair (59), and lung transplantation. It is typically classified as subvalvular, valvular, or supravalvular. The dynamic form of RVOT obstruction occurs in a setting of reduced preload and hypertrophied RV, exacerbated by inotropic drugs (60). It has been observed in biventricular hypertrophic cardiomyopathy (61) and after lung transplantation (62). The diagnosis can be established by right ventricular catheterization and by TEE (62) (Figs. 9.35–9.37).

D. Mitral Valve Fluttering from Aortic Regurgitation

During diastole, the presence of a significant aortic regurgitant jet may interfere with the full opening of the MV anterior leaflet and cause diastolic high-frequency fluttering best demonstrated by M-mode. This may be secondary to a severe jet of aortic regurgitation (AR), or with milder jets eccentrically directed towards the base of the anterior mitral leaflet. In the presence of severe AR, it will be associated with premature closure of the MV. It will not be observed if the leaflet is sclerotic and rigid or if the regurgitant jet is directed towards the ventricular septum (63) (Fig. 9.38) (see Chapter 15).

E. Midsystolic Pulmonary Valve Closure in Pulmonary Hypertension

The presence of a mid-systolic decrease or a notch in Doppler flow or using M-mode through the pulmonary valve is a useful sign indicative of severe pulmonary hypertension (Fig. 9.39). It is thought to be secondary to the reflected wave due to elevated distal pulmonary artery pressure and vascular resistance (64). However, it

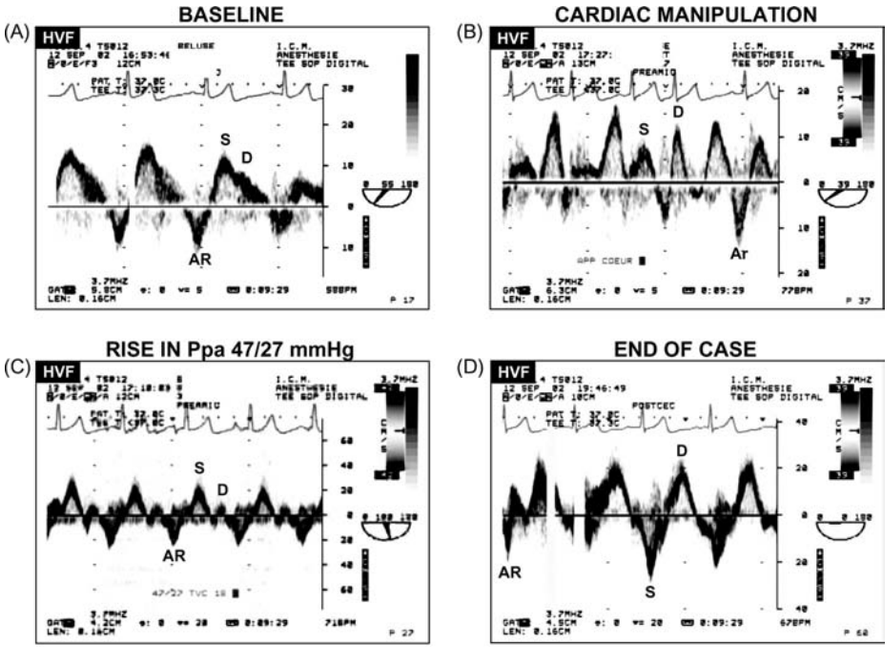

Figure 9.33 Worsening right ventricular diastolic function during mitral valve repair in a 69-year-old man. (A) The hepatic venous flow (HVF) S/D ratio is normal with increased atrial reversal (AR) velocities. (B) During manual cardiac manipulations of the heart, the S velocity is reduced. (C) With further elevation of the pulmonary pressure (Ppa) to 47/27, the AR velocity increases in relation to the S-wave. (D) Finally at the end of the procedure, systolic flow reversal is observed.

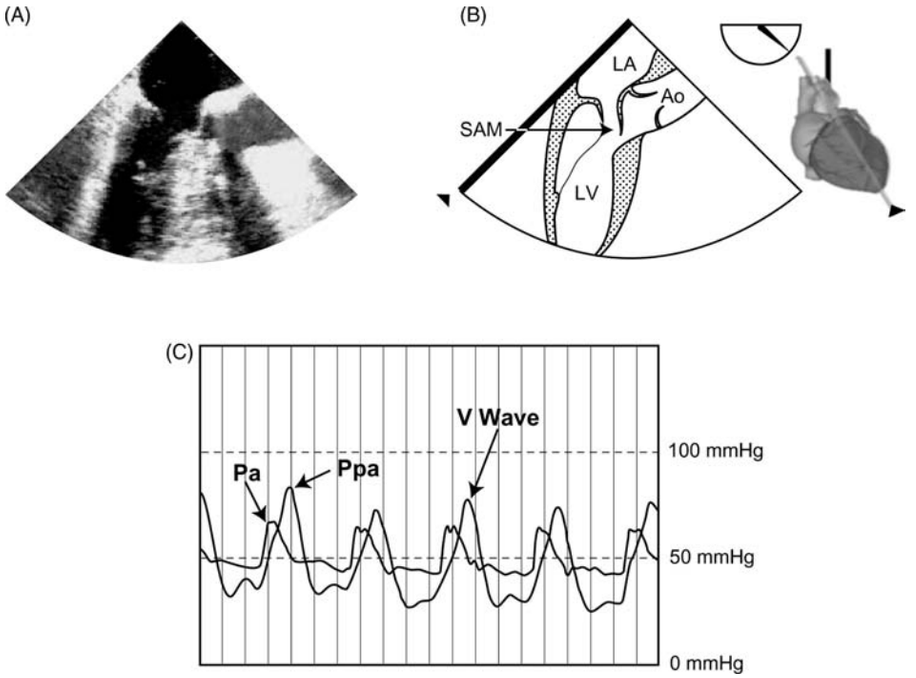

Figure 9.34 Left ventricular outflow tract obstruction in a 53-year-old man after aortic valve replacement. (A, B) The mid-esophageal long-axis view showed the LVOT obstruction secondary to left ventricular septal hypertrophy. (C) Systemic hypotension was associated with the appearance of a giant "V" wave on the wedged pulmonary artery pressure (Ppa) tracing occurred as the patient was weaned from cardiopulmonary bypass. The "V" wave was secondary to mitral valve regurgitation from abnormal systolic anterior motion (SAM). This patient did not respond to medical therapy and underwent mitral valve replacement (Ao, aorta; LA, left atrium; LV, left ventricle; Pa, arterial pressure).

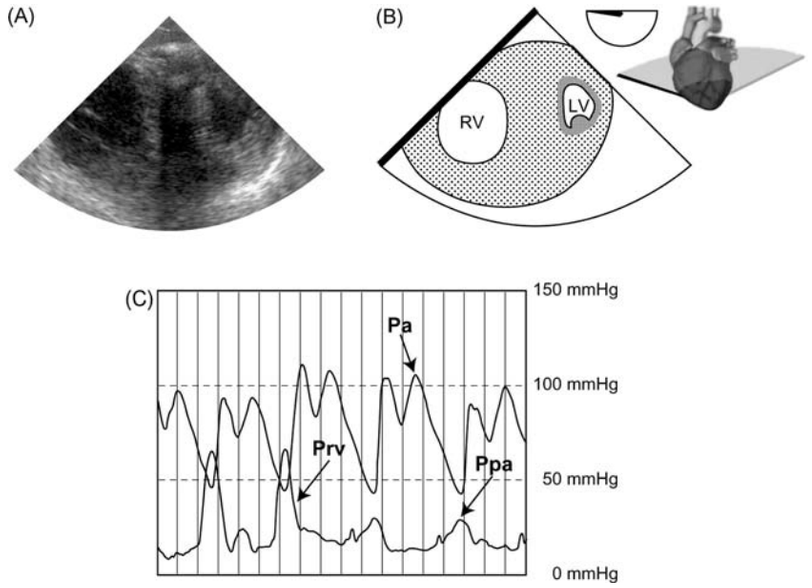

Figure 9.35 Right ventricular outflow tract obstruction in a 75-year-old man after coronary revascularization and aortic valve replacement. The procedure was complicated by two failed attempt of weaning from cardiopulmonary bypass requiring intra-aortic balloon counterpulsation. (A, B) Transgastric mid-papillary short-axis view revealed a dilated and hypertrophied right ventricle (RV). Unexplained acute right heart failure was present without pulmonary hypertension. (C) Pulmonary artery pressure (Ppa) was 34/22 mmHg and right atrial pressure 20 mmHg. However, a significant systolic pressure gradient between the right ventricular pressure (Prv) and the pulmonary artery was present (LV, left ventricle; Pa, arterial pressure).

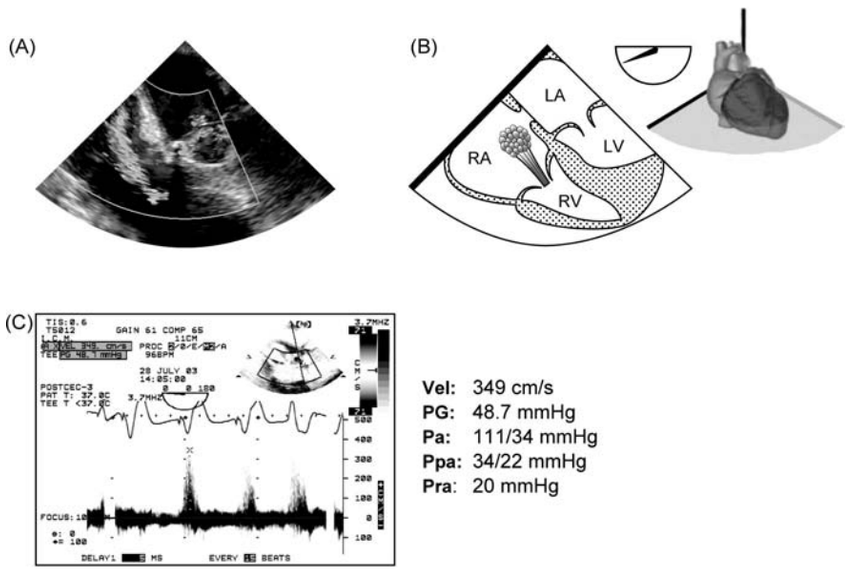

Figure 9.36 Right ventricular outflow tract obstruction. Same patient as in Fig. 9.35. (A, B) The right ventricular systolic pressure is estimated at 68.7 mmHg based on a right atrial pressure (Pra) of 20 mmHg and a right ventricle (RV) to right atrium (RA) pressure gradient (PG) of 48.7 mmHg from a tricuspid regurgitant velocity (Vel) of 349 cm/sec. The pulmonary artery pressure (Ppa) was directly measured at 34/22 mmHg. This would yield an outflow tract dynamic obstruction PG of 34.7 mmHg confirmed by directed right ventricular pressure tracing (see previous figure). The obstruction was exacerbated by intravenous milrinone and dopamine which were promptly discontinued. Weaning from cardiopulmonary bypass was then successful. The next day, all vasoactive medications were stopped and no residual right ventricular to pulmonary artery pressure gradient was present (LA, left atrium; LV, left ventricle; Pa, arterial pressure).

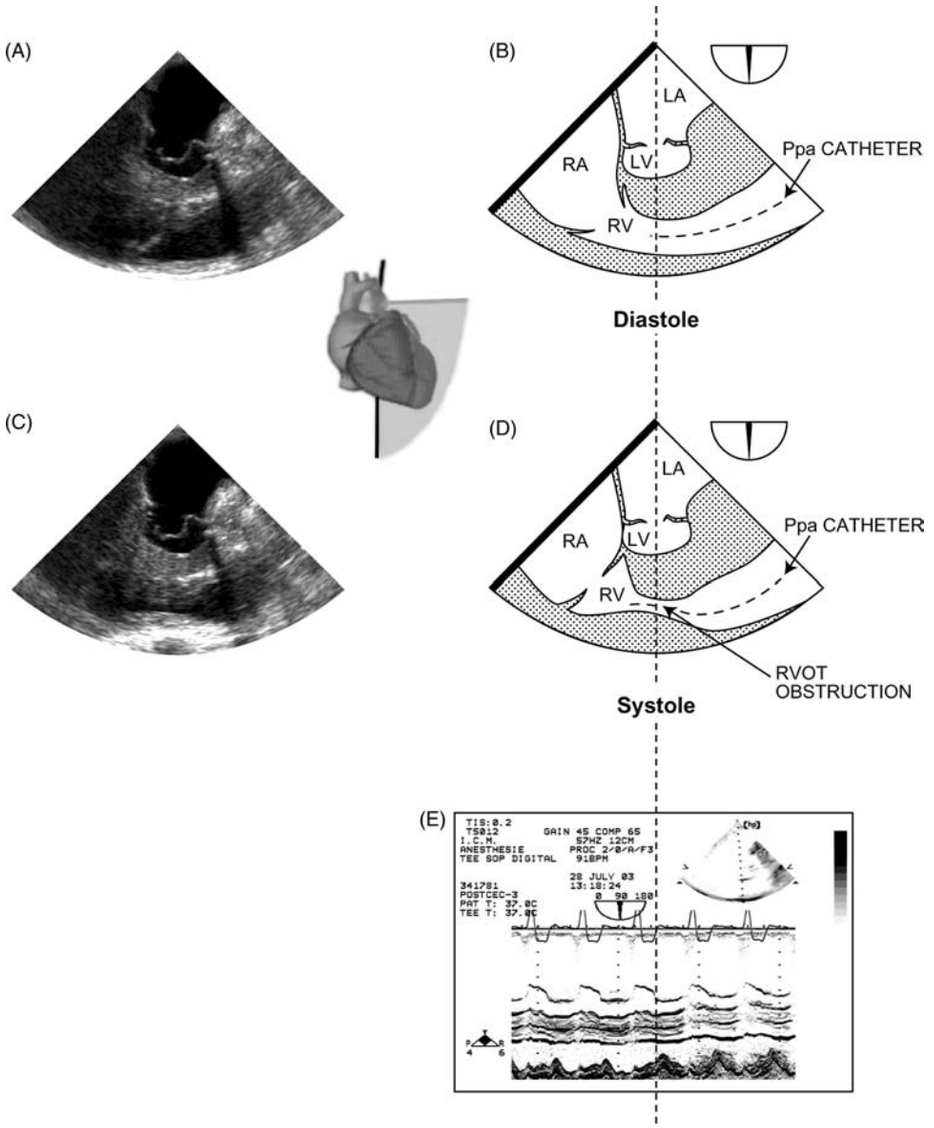

Figure 9.37 Right ventricular outflow tract obstruction. Same patient as in Fig. 9.35. The mid-esophageal right ventricular inflow–outflow view exam showed dynamic right ventricular outflow tract (RVOT) obstruction using 2D (A–D) and M-mode echocardiography (E) (LA, left atrium; LV, left ventricle; Ppa, pulmonary artery pressure; RA, right atrium; RV, right ventricle).

has also been reported in patients with pulmonary artery dilatation without pulmonary hypertension (65).

VII. PULMONARY THROMBOEMBOLISM

Pulmonary thromboembolism can be associated with severe right ventricular systolic and diastolic dysfunction. It can be due to *in situ* thrombus or thromboembolic material from deep venous thrombosis (Fig. 9.40) (66) or nonthrombotic from CO_2 (Fig. 9.41) (67), air (Fig. 9.42), or fat emboli as it may occur during orthopedic procedures (68). Echocardiography is considered pivotal in the evaluation of hemodynamically unstable patients suspected of pulmonary embolism (69) because it helps stratify those with evidence of right ventricular involvement. Such patients with right ventricular dysfunction or enlargement are at increased risk of hemodynamic instability and death. In the presence of hemodynamic instability, thrombolytic therapy, or surgical embolectomy may be lifesaving. Echocardiographic observations in pulmonary embolism include thrombus in transit in the RA, RV, or pulmonary artery, a dilated main

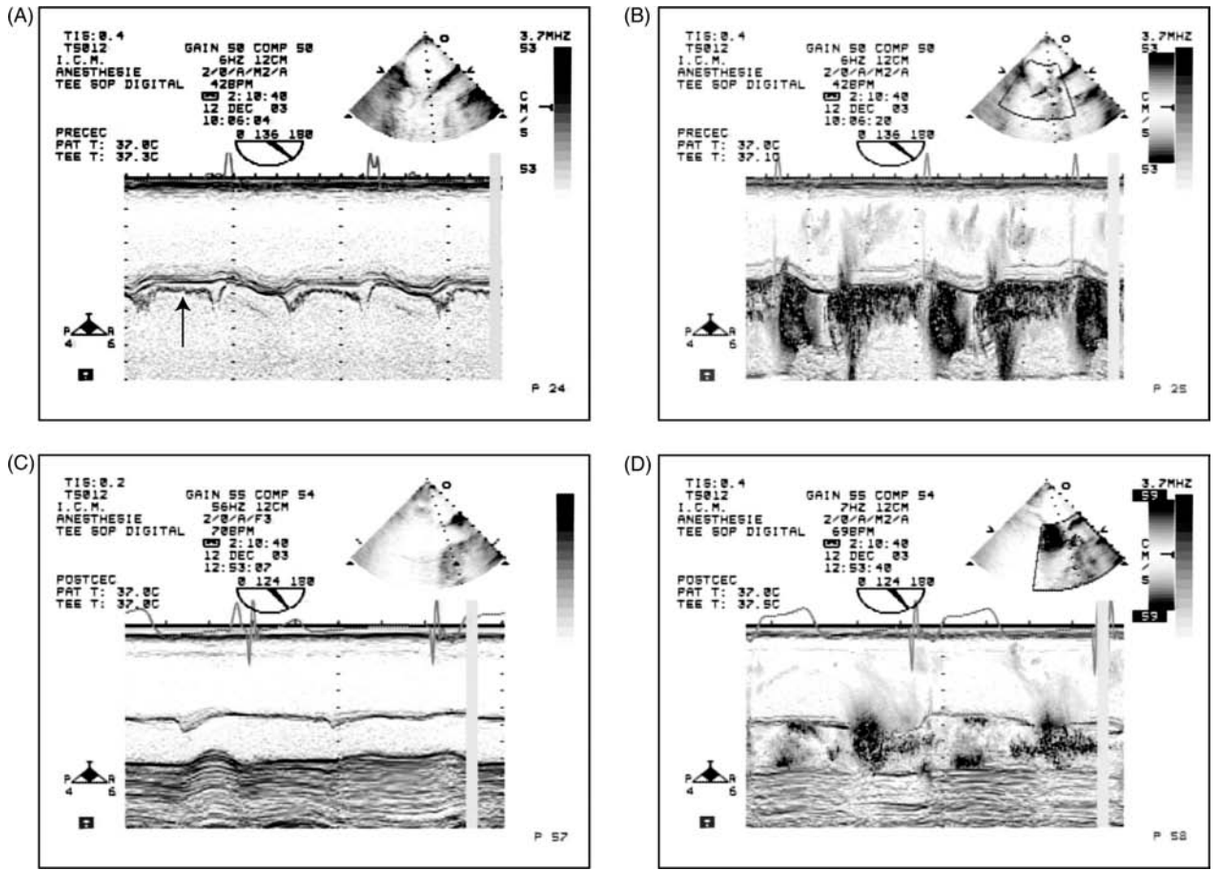

Figure 9.38 Mitral valve fluttering in a 56-year-old man being operated on for severe aortic regurgitation. (A) Fluttering of the anterior mitral leaflet (arrow) is seen using M-mode. (B) Aortic regurgitation on color M-mode. (C) After aortic valve replacement, the fluttering of the anterior mitral leaflet has disappeared. (D) The aortic regurgitation is now trivial.

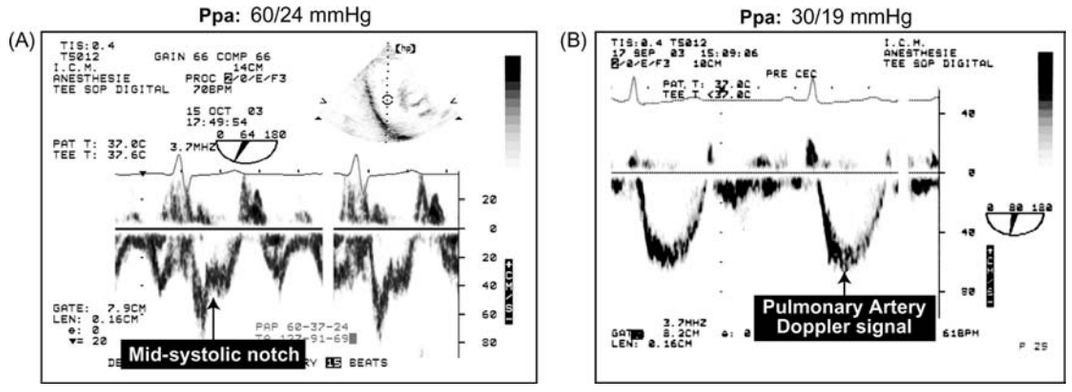

Figure 9.39 (A) Pulmonary hypertension in a 70-year-old man hemodynamically unstable with a pulmonary artery pressure (Ppa) of 60/24 mmHg. The pulmonary artery signal has a mid-systolic notch. (B) For comparison, a normal laminar pulmonary artery Doppler signal is shown from a 64-year-old woman before coronary revascularisation with a Ppa of 30/19 mmHg.

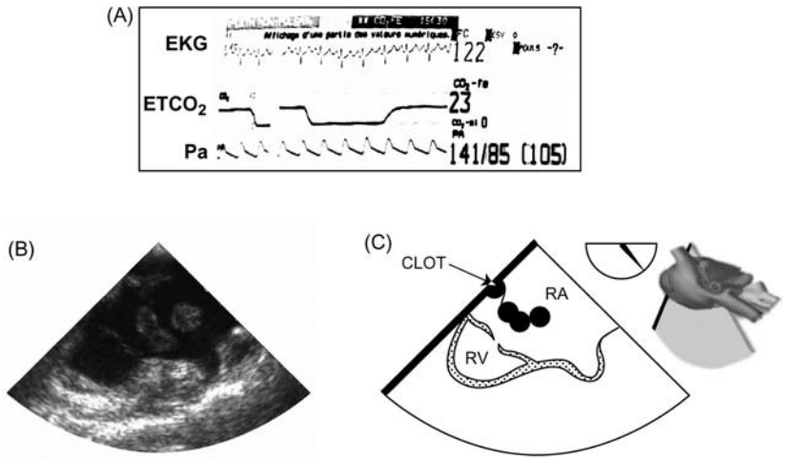

Figure 9.40 Thrombotic pulmonary emboli in a 68-year-old woman with hypotension and shortness of breath 4 weeks after a brain meningioma removal. (A) Hemodynamic data: heart rate of 122 beats/min, arterial pressure (Pa) of 141/85 mmHg on noradrenaline at 10 μgmin with end-tidal CO_2 ($ETCO_2$) of 22 mmHg. Note the peaked P-waves on the electrocardiogram (EKG) waveform suggesting right atrial dilatation. (B, C) Highly mobile clots floating in the right atrium (RA) are seen on a mid-esophageal 120° view (RV, right ventricle). (Photo B courtesy of Dr. Guy Cousineau.)

pulmonary artery, RV, RA, and inferior vena cava, in conjunction with reduced LV size, tricuspid regurgitation (TR), and abnormal flattening of the ventricular septum. In patients with gaseous embolism, air bubbles will tend to localize to the most vertically superior part of the heart which is the pulmonic valve and the atrial septum in a supine patient (Fig. 9.42).

VIII. CONCLUSION

In summary, TEE is an important tool for evaluation of global left and right ventricular systolic and diastolic function. It provides a unique and rapid diagnostic tool that has been, so far, unsurpassed in the setting of hemodynamic instability.

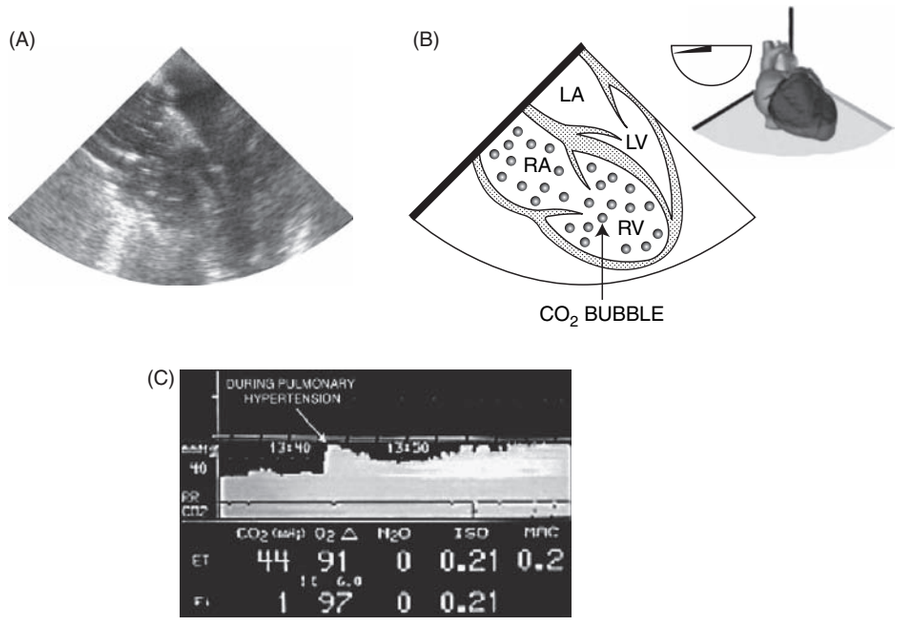

Figure 9.41 Carbon dioxide (CO_2) embolism in a 69-year-old man undergoing laparoscopic saphenectomy who suddenly became hemodynamically unstable. (A, B) A mid-esophageal four-chamber view showed the appearance of bubbles in the right atrium (RA) and right ventricle (RV) originating from the inferior vena cava. This was associated with right cardiac chamber dilatation. (C) The hemodynamic instability coincide with an abrupt rise in end-tidal CO_2 (LA, left atrium; LV, left ventricle). [Adapted from Martineau et al. (67).]

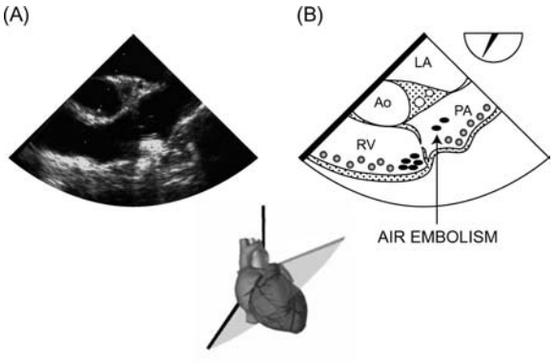

Figure 9.42 Air embolism in a 46-year-old woman hemodynamically unstable during spinal surgery in a ventral position. (A, B) She was turned back to a supine position and a mid-esophageal right ventricular outflow view revealed the residual presence of air bubbles on the most anterior aspect of the right ventricle (RV), pulmonary artery (PA) and on both sides of the anterior pulmonic valve (Ao, aorta; LA, left atrium).

REFERENCES

1. Practice guidelines for perioperative transesophageal echocardiography. A report by the American Society of Anesthesiologists and the Society of Cardiovascular Anesthesiologists Task Force on Transesophageal Echocardiography. Anesthesiology 1996; 84:986–1006.
2. Schiller NB, Shah PM, Crawford M et al. Recommendations for quantitation of the left ventricle by two-dimensional echocardiography. American Society of Echocardiography Committee on Standards, Subcommittee on Quantitation of Two-Dimensional Echocardiograms. J Am Soc Echocardiogr 1989; 2:358–367.
3. Emilsson K, Alam M, Wandt B. The relation between mitral annulus motion and ejection fraction: a nonlinear function. J Am Soc Echocardiogr 2000; 13:896–901.
4. Alam M, Wardell J, Andersson E et al. Effects of first myocardial infarction on left ventricular systolic and diastolic function with the use of mitral annular velocity determined by pulsed wave doppler tissue imaging. J Am Soc Echocardiogr 2000; 13:343–352.
5. Gorcsan J III, Denault A, Gasior TA et al. Rapid estimation of left ventricular contractility from end-systolic relations by echocardiographic automated border detection and femoral arterial pressure. Anesthesiology 1994; 81:553–562.
6. Denault AY, Gorcsan J III, Mandarino WA et al. Left ventricular performance assessed by echocardiographic automated border detection and arterial pressure. Am J Physiol 1997; 272:H138–H147.
7. Vieillard-Baron A, Augarde R, Prin S et al. Influence of superior vena caval zone condition on cyclic changes in right ventricular outflow during respiratory support. Anesthesiology 2001; 95:1083–1088.
8. Leung JM, Levine EH. Left ventricular end-systolic cavity obliteration as an estimate of intraoperative hypovolemia. Anesthesiology 1994; 81:1102–1109.
9. Tavernier B, Makhotine O, Lebuffe G et al. Systolic pressure variation as a guide to fluid therapy in patients with sepsis-induced hypotension. Anesthesiology 1998; 89:1313–1321.
10. Tousignant CP, Walsh F, Mazer CD. The use of transesophageal echocardiography for preload assessment in critically ill patients. Anesth Analg 2000; 90(2):351–355.
11. Feissel M, Michard F, Mangin I et al. Respiratory changes in aortic blood velocity as an indicator of fluid responsiveness in ventilated patients with septic shock. Chest 2001; 119:867–873.
12. Kusumoto FM, Muhiudeen IA, Kuecherer HF et al. Response of the interatrial septum to transatrial pressure gradients and its potential for predicting pulmonary capillary wedge pressure: an intraoperative study using transesophageal echocardiography in patients during mechanical ventilation. J Am Coll Cardiol 1993; 21:721–728.
13. Mulvagh S, Quinones MA, Kleiman NS et al. Estimation of left ventricular end-diastolic pressure from Doppler transmitral flow velocity in cardiac patients independent of systolic performance. J Am Coll Cardiol 1992; 20:112–119.
14. Nomura M, Hillel Z, Shih H et al. The association between Doppler transmitral flow variables measured by transesophageal echocardiography and pulmonary capillary wedge pressure. Anesth Analg 1997; 84:491–496.
15. Appleton CP, Galloway JM, Gonzalez MS et al. Estimation of left ventricular filling pressures using two-dimensional and Doppler echocardiography in adult patients with cardiac disease. Additional value of analyzing left atrial size, left atrial ejection fraction and the difference in duration of pulmonary venous and mitral flow velocity at atrial contraction. J Am Coll Cardiol 1993; 22:1972–1982.
16. Kimura K, Murata K, Tanaka N et al. The importance of pulmonary venous flow measurement for evaluating left ventricular end-diastolic pressure in patients with coronary artery disease in the early stage of diastolic dysfunction. J Am Soc Echocardiogr 2001; 14:987–993.
17. Kuecherer HF, Muhiudeen IA, Kusumoto FM et al. Estimation of mean left atrial pressure from transesophageal pulsed doppler echocardiography of pulmonary venous flow. Circulation 1990; 82:1127–1139.
18. Girard F, Couture P, Boudreault D et al. Estimation of the pulmonary capillary wedge pressure from transesophageal pulsed Doppler echocardiography of pulmonary venous flow: influence of the respiratory cycle during mechanical ventilation. J Cardiothorac Vasc Anesth 1998; 12:16–21.
19. Lattik R, Couture P, Denault AY et al. Mitral Doppler indices are superior to two-dimensional and conventional hemodynamic indices to predict fluid responsiveness. Anesth Analg 2002; 94:1092–1099.
20. Nagueh SF, Middleton KJ, Kopelen HA et al. Doppler tissue imaging: a noninvasive technique for evaluation of left ventricular relaxation and estimation of filling pressures. J Am Coll Cardiol 1997; 30:1527–1533.
21. Kim YJ, Sohn DW. Mitral annulus velocity in the estimation of left ventricular filling pressure: prospective study in 200 patients. J Am Soc Echocardiogr 2000; 13:980–985.
22. Firstenberg MS, Levine BD, Garcia MJ et al. Relationship of echocardiographic indices to pulmonary capillary wedge

pressures in healthy volunteers. J Am Coll Cardiol 2000; 36:1664–1669.
23. Garcia MJ, Ares MA, Asher C et al. An index of early left ventricular filling that combined with pulsed Doppler peak E velocity may estimate capillary wedge pressure. J Am Coll Cardiol 1997; 29:448–454.
24. Sunagawa K, Maughan WL, Sagawa K. Optimal arterial resistance for the maximal stroke work studied in isolated canine left ventricle. Circ Res 1985; 56:586–595.
25. Gorcsan J, Gasior TA, Mandarino WA et al. Assessment of the immediate effects of cardiopulmonary bypass on left ventricular performance by on-line pressure–area relations. Circulation 1994; 89:180–190.
26. Simonson JS, Schiller NB. Descent of the base of the left ventricle: an echocardiographic index of left ventricular function. J Am Soc Echocardiogr 1989; 2:25–35.
27. Tei C, Dujardin KS, Hodge DO et al. Doppler index combining systolic and diastolic myocardial performance: clinical value in cardiac amyloidosis. J Am Coll Cardiol 1996; 28:658–664.
28. Eidem BW, O'Leary PW, Tei C, Seward JB. Usefulness of the myocardial performance index for assessing right ventricular function in congenital heart disease. Am J Cardiol 2000; 86:654–658.
29. Moller JE, Sondergaard E, Poulsen SH et al. Serial Doppler echocardiographic assessment of left and right ventricular performance after a first myocardial infarction. J Am Soc Echocardiogr 2001; 14:249–255.
30. Costachescu T, Denault AY, Guimond JG et al. The hemodynamically unstable patient in the intensive care unit: hemodynamic vs. transesophageal echocardiographic monitoring. Crit Care Med 2002; 30:1214–1223.
31. Pai RG, Bansal RC, Shah PM. Doppler-derived rate of left ventricular pressure rise. Its correlation with the postoperative left ventricular function in mitral regurgitation. Circulation 1990; 82:514–520.
32. Reichert CL, Visser CA, van den Brink RB et al. Prognostic value of biventricular function in hypotensive patients after cardiac surgery as assessed by transesophageal echocardiography. J Cardiothorac Vasc Anesth 1992; 6:429–432.
33. Maslow AD, Regan MM, Panzica P et al. Precardiopulmonary bypass right ventricular function is associated with poor outcome after coronary artery bypass grafting in patients with severe left ventricular systolic dysfunction. Anesth Analg 2002; 95:1507–1518.
34. Eddy AC, Rice CL, Anardi DM. Right ventricular dysfunction in multiple trauma victims. Am J Surg 1988; 155:712–715.
35. Mitsuo T, Shimazaki S, Matsuda H. Right ventricular dysfunction in septic patients. Crit Care Med 1992; 20:630–634.
36. Davila-Roman VG, Waggoner AD, Hopkins WE, Barzilai B. Right ventricular dysfunction in low output syndrome after cardiac operations: assessment by transesophageal echocardiography. Ann Thorac Surg 1995; 60:1081–1086.
37. Wranne B, Pinto FJ, Hammarstrom E et al. Abnormal right heart filling after cardiac surgery: time course and mechanisms. Br Heart J 1991; 66:435–442.
38. Appleton CP, Hatle LK, Popp RL. Superior vena cava and hepatic vein Doppler echocardiography in healthy adults. J Am Coll Cardiol 1987; 10:1032–1039.
39. Pinto FJ, Wranne B, St Goar FG et al. Hepatic venous flow assessed by transesophageal echocardiography. J Am Coll Cardiol 1991; 17:1493–1498.
40. Pinto FJ, Wranne B, St Goar FG et al. Systemic venous flow during cardiac surgery examined by intraoperative transesophageal echocardiography. Am J Cardiol 1992; 69:387–393.
41. Bernard F, Denault A, Babin D et al. Diastolic dysfunction is predictive of difficult weaning from cardiopulmonary bypass. Anesth Analg 2001; 92:291–298.
42. Khouri SJ, Maly GT, Suh DD, Walsh TE. A practical approach to the echocardiographic evaluation of diastolic function. J Am Soc Echocardiogr 2004; 17:290–297.
43. Ozer N, Tokgozoglu L, Coplu L, Kes S. Echocardiographic evaluation of left and right ventricular diastolic function in patients with chronic obstructive pulmonary disease. J Am Soc Echocardiogr 2001; 14:557–561.
44. Caso P, Galderisi M, Cicala S et al. Association between myocardial right ventricular relaxation time and pulmonary arterial pressure in chronic obstructive lung disease: analysis by pulsed Doppler tissue imaging. J Am Soc Echocardiogr 2001; 14:970–977.
45. Denault A, Couture P, Perrault LP, Tardif JC. Diagnosis, predictors, mechanisms, and treatment of hemodynamic instability in cardiac surgery: research perspective at the Montreal Heart Institute. In: Pandalai SG, ed. Recent Research Developments in Anesthesia and Analgesia. Kerala: Transworld Research Network, 2003:25–43.
46. Freeman WK, Schaff HV, Khandheria BK et al. Intraoperative evaluation of mitral valve regurgitation and repair by transesophageal echocardiography: incidence and significance of systolic anterior motion. J Am Coll Cardiol 1992; 20:599–609.
47. Pollick C, Morgan CD, Gilbert BW et al. Muscular subaortic stenosis: the temporal relationship between systolic anterior motion of the anterior mitral leaflet and the pressure gradient. Circulation 1982; 66:1087–1094.
48. Heidenreich PA, Stainback RF, Redberg RF et al. Transesophageal echocardiography predicts mortality in critically ill patients with unexplained hypotension. J Am Coll Cardiol 1995; 26:152–158.
49. Gouello JP, Bouachour G, Vincent JF et al. Detection of left cardiopathy using echocardiography during acute respiratory failure in chronic respiratory insufficiency. Rev Mal Respir 1995; 12:145–150.
50. Murtha W, Guenther C. Dynamic left ventricular outflow tract obstruction complicating bilateral lung transplantation. Anesth Analg 2002; 94:558–559.
51. Di Chiara A, Plewka M, Fioretti PM. Systolic anterior movement of mitral valve during acute apical myocardial infarction: an unusual mechanism of acute mitral regurgitation. J Am Soc Echocardiogr 1999; 12:1117–1121.
52. Morewood GH, Weiss SJ. Intra-aortic balloon pump associated with dynamic left ventricular outflow tract obstruction

after valve replacement for aortic stenosis. J Am Soc Echocardiogr 2000; 13:229–231.
53. Murtha W, Guenther C. Dynamic left ventricular outflow tract obstruction complicating bilateral lung transplantation. Anesth Analg 2002; 94:558–559.
54. Doshi SN, Kim MC, Sharma SK, Fuster V. Images in cardiovascular medicine. Right and left ventricular outflow tract obstruction in hypertrophic cardiomyopathy. Circulation 2002; 106:e3–e4.
55. Agarwal S, Choudhary S, Saxena A et al. Giant pulmonary artery aneurysm with right ventricular outflow tract obstruction. Indian Heart J 2002; 54:77–79.
56. Tardif JC, Taylor K, Pandian NG et al. Right ventricular outflow tract and pulmonary artery obstruction by postoperative mediastinal hematoma: delineation by multiplane transesophageal echocardiography. J Am Soc Echocardiogr 1994; 7:400–404.
57. Dall'Agata A, Cromme-Dijkhuis AH, Meijboom FJ et al. Use of three-dimensional echocardiography for analysis of outflow obstruction in congenital heart disease. Am J Cardiol 1999; 83:921–925.
58. Bennink GB, Hitchcock FJ, Molenschot M et al. Aneurysmal pericardial patch producing right ventricular inflow obstruction. Ann Thorac Surg 2001; 71:1346–1347.
59. Basaria S, Denktas AE, Ghani M, Thandroyen F. Ventricular septal defect patch causing right ventricular inflow tract obstruction. Circulation 1999; 100:e12–e13.
60. Kirshbom PM, Tapson VF, Harrison JK et al. Delayed right heart failure following lung transplantation. Chest 1996; 109:575–577.
61. Stierle U, Sheikhzadeh A, Shakibi JG et al. Right ventricular obstruction in various types of hypertrophic cardiomyopathy. Jpn Heart J 1987; 28:115–125.
62. Gorcsan J, Reddy SC, Armitage JM, Griffith BP. Acquired right ventricular outflow tract obstruction after lung transplantation: diagnosis by transesophageal echocardiography. J Am Soc Echocardiogr 1993; 6:324–326.
63. Winsberg F, Gabor GE, Hernberg JG, Weiss B. Fluttering of the mitral valve in aortic insufficiency. Circulation 1970; 41:225–229.
64. Weyman AE, Dillon JC, Feigenbaum H, Chang S. Pulmonary valve echo motion in pulmonary regurgitation. Br Heart J 1975; 37:1184–1190.
65. Bauman W, Wann LS, Childress R et al. Mid systolic notching of the pulmonary valve in the absence of pulmonary hypertension. Am J Cardiol 1979; 43:1049–1052.
66. Leibowitz D. Role of echocardiography in the diagnosis and treatment of acute pulmonary thromboembolism. J Am Soc Echocardiogr 2001; 14:921–926.
67. Martineau A, Arcand G, Couture P et al. Transesophageal echocardiographic diagnosis of carbon dioxide embolism during minimally invasive saphenous vein harvesting and treatment with inhaled epoprostenol. Anesth Analg 2003; 96:962–964.
68. Parmet JL, Horrow JC, Pharo G et al. The incidence of venous emboli during extramedullary guided total knee arthroplasty. Anesth Analg 1995; 81:757–762.
69. Wood KE. Major pulmonary embolism: review of a pathophysiologic approach to the golden hour of hemodynamically significant pulmonary embolism. Chest 2002; 121:877–905.